LAPPEENRANTA UNIVERSITY OF TECHNOLOGY
Faculty of Technology
Degree Programme of Chemical and Process Engineering

MODELING OF GOLD CYANIDATION

by

Waroonkarn Srithammavut

Master of Science (Technology) Thesis

Examiners: Professor Ilkka Turunen
D. Sc. Arto Laari

Supervisors: Pia Sinisalo
Pasi Viinikka
Jussi Vaarno

ACKNOWLEDGMENT

This work was supported by Outotec Research Oy (ORC) in Pori and Lappeenranta University of Technology (LUT). It is a pleasure to convey my gratitude to all of people involved in this study.

In the first place I would like to express my sincere appreciation to Professor Ilkka Turunen (LUT) for his support and unflinching encouragement during thesis's work. I am also indebted to Arto Laarti (LUT) for his valuable advice in science discussion, assistance about Modest computer software and revise the thesis.

I gratefully acknowledge supervisors, Pia Sinisalo (ORC), Pasi Viinikka (ORC) and Jussi Vaarno (ORC) for their technical comments, advice, guidance, patience to answer some unintelligent questions and revise the thesis. I also extend my appreciation to Timo Kankaanpää (ORC) for revise my thesis and assistance in various ways. I hope to keep up our collaboration in the future.

I would like to acknowledge my family for all their love and moral support throughout this work. Finally, many thanks go to all of my lovely friends who always listen to my problems and cheer me up until the last minute of this work.

ABSTRACT

Lappeenranta University of Technology
Department of Chemical Technology

Waroonkarn Srithammavut

Modeling of gold cyanidation

Master of Science (Technology) Thesis

2008

93 pages, 43 figures, 9 tables and 1 appendix

Examiner: Professor Ilkka Turunen
D.Sc. Arto Laari

Keywords: Gold cyanidation; Leaching; Reaction kinetics; Modeling

The chemistry of gold dissolution in alkaline cyanide solution has continually received attention and new rate equations expressing the gold leaching are still developed. The effect of leaching parameters on gold cyanidation is studied in this work in order to optimize the leaching process. A gold leaching model, based on the well-known shrinking-core model, is presented in this work. It is proposed that the reaction takes place at the reacting particle surface which is continuously reduced as the reaction proceeds. The model parameters are estimated by comparing experimental data and simulations. The experimental data used in this work was obtained from Ling *et al*. (1996) and de Andrade Lima and Hodouin (2005). Two different rate equations, where the unreacted amount of gold is considered in one equation, are investigated. In this work, it is presented that the reaction at the surface is the rate controlling step since there is no internal diffusion limitation. The model considering the effect of non-reacting gold shows that the reaction orders are consistent with the experimental observations reported by Ling *et al*. (1996) and de Andrade Lima and Hodouin (2005). However, it should be noted that the model obtained in this work is based on assumptions of no side reactions, no solid-liquid mass transfer resistances and no effect from temperature.

TABLE OF CONTENTS

TABLE OF FIGURES

LIST OF TABLES

NOMENCLATURE

Roman Letters

A	surface area of gold	[m^2]
A_i	surface area of one particle during leaching	[m^2]
A_r	reacting surface area of particles	[m^2]
A_{r_i}	inner surface area of passive layer	[m^2]
A_{r_o}	outer surface area of passive layer	[m^2]
a	specific interfacial area	[$m^2\ m_R^{-3}$]
b	Freundlich adsorption constant	[-]
C	concentration in spherical diffusion layer	[mol m_L^{-3}]
C_{Au}	gold concentration in particles	[mol m_R^{-3}]
$C_{Au,ini}$	gold initial concentration in particles	[mol m_R^{-3}]
C_{Au}^{∞}	gold concentration in particles after infinite leaching time	[mol m_R^{-3}]
$C_{Au,C}$	gold concentration in carbon	[mol m^{-3}]
$C_{Au,L}^{ini}$	gold concentration in solution at initial time	[mol m_L^{-3}]
$C_{Au,L}$	gold concentration in solution	[mol m_L^{-3}]
$C_{Au,L}(t)$	gold concentration in solution at time t	[mol m_L^{-3}]
$C_{Au,s}$	surface concentration of gold in particles	[mol m^{-2}]
C_{CN^-}	cyanide concentration	[mol m_L^{-3}]
C_i	concentration in solution at inner passive layer	[mol m_L^{-3}]
C_o	concentration in solution at outer passive layer	[mol m_L^{-3}]

C_{O_2}	oxygen concentration	[mol m_L^{-3}]
$C_{O_2,s}$	dissolved oxygen concentration at the reacting surface	[mol m_L^{-3}]
c_1, c_2	coefficients in Equation (27)	
c_3, c_4	coefficients in Equation (30)	
D_{CN^-}	diffusion coefficient of cyanide	[m^2 s^{-1}]
D_e	effective diffusivity in particles	[m^2 s^{-1}]
D_m	molecular diffusivity	[m^2 s^{-1}]
D_{O_2}	diffusion coefficient of oxygen	[m^2 s^{-1}]
$\bar{d}$	average diameter of particles	[m]
d_D	impeller diameter	[m]
d_P	particle diameter	[m]
d_T	tank diameter	[m]
E°	standard reaction potential	[V]
E_h	reduction potential	[V]
F	the Faraday constant (96,485.34)	[C mol^{-1}]
Ga	Galileo number, $d_P^3 \Delta\rho g \rho_L^2/\mu$	[-]
g	gravitational acceleration	[m s^{-2}]
H	distance traveled by eddy in concentrated boundary layer surrounding the particle	[m]
k	overall rate constant in Equation (25) and (26)	
k_1	overall rate constant in Equations (42), (52) and (54)	[$(mol/m^3)^{-2.35}$ h^{-1}, $(mol/m^3)^{0.668}$ h^{-1}]
k_2	overall rate constant in Equations (43), (53) and (55)	[$(mol/m^3)^{-2.731}$ h^{-1}, $(mol/m^3)^{-2.011}$ h^{-1}]

k_a	rate constant for anodic half-reaction	[C m mol^{-1} s^{-1}]
k_{ads}	rate constant for gold adsorption	[s^{-1}]
k_{CN^-}	rate constant in Equation (23)	[s^{-1}]
k_c	rate constant for cathodic half-reaction	[C m mol^{-1} s^{-1}]
k_L	liquid-gas mass transfer coefficient	[m s^{-1}]
k_La	volumetric mass transfer coefficient	[s^{-1}]
k_{O_2}	rate constant in Equation (24)	[s^{-1}]
k_{SL}	solid-liquid mass transfer coefficient	[m s^{-1}]
m	constant in Equation (33)	[-]
m_{T}	total mass of particles	[kg]
N	stirrer speed	[s^{-1}]
$\dot{N}_{O_2}$	diffusion rate of oxygen	[mol s^{-1}]
N_{Au}	amount of gold in particles	[mol]
N_{Po}	power number, $P/\rho N^3 d_{\mathrm{D}}{}^5$	[-]
n	number of particles per volume	[m_R^{-3}]
n'	Freundlich exponent	[-]
P	power input under gassed conditions	[W]
Re_{N}	Reynolds number based on impeller diameter, $Nd_{\mathrm{D}}{}^2\rho/\mu$	[-]
Re_{T}	Reynolds number based on tank diameter, $NT^2\rho/\mu$	[-]
Re_{P}	Reynolds number based on particle diameter, $d_{\mathrm{P}}d_{\mathrm{T}}\omega\pi/\mu$	[-]
Re_{ε}	Reynolds number based on Kolmogoroff's theory of Isotropic turbulence, $(\varepsilon d_{\mathrm{P}}{}^4/\upsilon^3)^{1/3}$	[-]
r	radial coordinate	[m]
r_{CN^-}	reaction rate for cyanide consumption in Equation (29)	[kg m^{-3} s^{-1}]
r_i	inner radius of passive layer	[m]

r_o	outer radius of passive layer	[m]
r_s	reaction rate at surface	[mol m^{-2} s^{-1}]
Sc	Schmidt number, $\mu/\rho D_m$	[-]
Sh_P	Sherwood number based on particle diameter, $k_{SL}d_P/D_m$	[-]
Sh_T	Sherwood number based on tank diameter, $k_{SL}d_T/D_m$	[-]
S_O	solubility of solute per 100 g of solute	[g g^{-1}]
t	time	[s]
U_G	superficial gas velocity	[m s^{-1}]
u_A	mass fraction of component A in solution	[kg A kg^{-1} solution]
V	volume of the liquid in the vessel	[m^3]
X	impeller clearance from the bottom of tank	[m]
x, y, z	exponents in Equation (33)	[-]

Greek letters

$\Delta\rho$	solid-liquid density different	[kg m^{-3}]
α	reaction order for cyanide	[-]
β	reaction order for oxygen	[-]
γ	reaction order for gold	[-]
δ	thickness of the Nernst boundary layer	[m]
δ_P	thickness of passive layer	[m]
η	reaction order in Equation (29)	[-]
θ	exponent for mean diameter of particles in Equation (27)	[-]
μ	dynamic viscosity	[Pa s]
μ_a	apparent viscosity according to the Ostwald de Waele model	[Pa s]

ρ	density	[kg m^{-3}]

Abbreviations

6FBT	flat blade turbine with 6 blades
B	baffled tank
CBT	curved blade turbine
CBP	curved blade paddle
CCL & Zn	solid-liquid separation and zinc precipitation
CIL	carbon-in-leach
CIP	carbon-in-pulp
FBP	flat blade paddle
ILR	InLine Leach Reactor
IS	inter-stage screens
MCMC	Marcov chain Monte Carlo
MISC	flotation and gravity concentrate
ORP	oxidation-reduction potential
PBT	pitched blade turbine
SCM	shrinking-core model
Two-6FBT	two stirrers of the type indicated
UB	unbaffled tank

1 INTRODUCTION

The chemical element gold, symbol Au, is classified as a noble metal due to its inertness to chemical reactions in non-complex media. It does, however, react with numerous reagents. It belongs to the same group as copper and silver in the periodic table and it is commonly found to be associated with these elements in rocks (Juvonen, 1999). Gold is also found in host minerals, typically such as calaverite ($AuTe_2$), montbroyite (Au_2Te_3) and sylvanite ($AuAgTe_4$), in varying concentrations and occurs in association with minerals, for example, sulfide and copper (Marsden and House, 1992). The average concentration of gold in earth's crust is 0.005 g/t, which is much lower than most other metals, for example, 0.07 g of silver/t and 50 g of copper/t. The gold content is dependent upon gold minerals as well as gold properties, for instance, electrum, specific gravity 16-19.3, is a mixture of silver and gold containing 45-75 % gold (Marsden and House, 1992). There are many possible methods to recover gold from ores such as leaching, gravity concentration and flotation. Leaching by cyanide solutions or gold cyanidation, however, has been the main metallurgical process for gold extraction for more than one century (de Andrade Lima and Hodouin, 2006).

Since the invention of the gold cyanidation process in 1887, its chemistry and leaching kinetics have been the subjects of considerable investigation and several theories have been proposed to explain the reaction mechanism. Various variables affecting gold cyanidation, such as dissolved oxygen concentration, free cyanide concentration, temperature, pH and particle size, have been studied. Their effects on the optimal gold conversion have been investigated since they could result in effective improvements at industrial scale, for instance the reduction of the operational cost. However, gold cyanidation is a complex system due to the fact that gold particles occur as alloys or compounds which are embedded in a mineral matrix and galvanic interaction can take place between the phases (de Andrade Lima and Hodouin, 2005). A number of these studies remain contradictory in their conclusions concerning the mechanism of dissolution. Some studies propose that

the diffusion of reactants to the gold surface controls the rate of reaction, while others claimed that the chemical reaction is slow (Crundwell *et al*, 1997).

For several years mathematical models have been extensively studied in order to obtain predictions for the kinetics of leaching reactions. A number of rate equations have been published based on different experimental conditions. Some of them are mechanistic rate equations and some are empirical ones. The first comprehensive study on the variation of the rate of gold dissolution with cyanide and oxygen concentration has been described since 1966. However, the limitation of the equation in the modeling of industrial gold cyanidation is due to the difficulty in measuring the exact surface area of gold in the ore and the Nernst boundary layer thickness (Ling *et al*, 1996). Additionally, numerous researchers have claimed that two expressions can be derived from the electrochemical mechanism of gold leaching and the shrinking core model with surface passivation (Crundwell *et al*, 1997). The gold leaching process often appears to be operated far from an optimum range. For example, excessive reagents (CN^- and O_2) consumption is expected and the behavior of the process is very dependent on feed mineralogy (Ling *et al*, 1996). Therefore, it is evident that a simple rate equation with a minimum number of adjustable parameters is still needed for the modeling of gold cyanidation.

In this work, the aim is to study the effect of leaching parameters on gold cyanidation and their limitations. The main purpose is to find the important factors which impact the reaction kinetics and to optimize the process of the gold leaching by gathering information from existing cyanide leaching processes. The Modest (Model Estimation) computer software is used for parameter estimation of the mechanistic mathematical models.

2 CHEMISTRY OF GOLD CYANIDATION

Gold cyanidation has been used as the principle gold extraction technique since the late 19th century. Cyanide is universally used because of its relatively low cost and great effectiveness for gold dissolution. Also, despite some concerns over the toxicity of cyanide, it can be applied with little risk to health and the environment.

2.1 Chemistry of cyanide solutions

Simple cyanide salts, for example, sodium cyanide (NaCN), potassium cyanide (KCN) and calcium cyanide [$Ca(CN_2)$], have been widely used as sources of cyanide leaching. They dissolve and ionize in water to form their respective metal cation and free cyanide ions (CN^-) as presented below:

$$NaCN \rightleftharpoons Na^+ + CN^- \quad (1)$$

Cyanide ions hydrolyze in water to form hydrogen cyanide (HCN) and hydroxyl (OH^-) ions which also increase pH. At pH about 9.3, half of total cyanide exists as hydrogen cyanide and half as free cyanide ions. At higher pH, the total cyanide greatly exists as free cyanide ions. Undesirable reactions might occur during leaching because hydrogen cyanide, as well as free cyanide, can be oxidized with oxygen to form cyanate (CNO^-) which does not dissolve gold and thus reduces the free cyanide concentration (Marsden and House, 1992).

$$CN^- + H_2O \rightleftharpoons HCN + OH^- \quad (2)$$

$$4HCN + 3O_2 \rightleftharpoons 4CNO^- + 2H_2O \quad (3)$$

$$3CN^- + 2O_2 + H_2O \rightleftharpoons 3CNO^- + 2OH^- \quad (4)$$

2.2 Gold dissolution

The oxidation of gold is a prerequisite for its dissolution in alkaline cyanide solution. Although gold is inert to oxidation, it is widely accepted that, in the presence of a suitable complex agent such as cyanide, gold is oxidized and

dissolved to form the stable complex ion [$Au(CN_2)^-$]. Oxygen is reduced and hydrogen peroxide is formed as an intermediate product in the first step and becomes the oxidizing agent in the second step, leading to the following chemical reactions which proceed in parallel (Marsden and House, 1992; Kondos *et al*, 1995; Ling *et al*, 1996; de Andrade Lima and Hodouin, 2005; Senanayake, 2005):

$$2Au + 4CN^- + O_2 + 2H_2O \rightarrow 2Au(CN)_2^- + H_2O_2 + 2OH^- \quad (5)$$

$$2Au + 4CN^- + H_2O_2 \rightarrow 2Au(CN)_2^- + 2OH^- \quad (6)$$

The summation of the two partial reactions is presented in Eq. (7), as proposed by Elsner:

$$4Au + 8CN^- + O_2 + 2H_2O \rightarrow 4Au(CN)_2^- + 4OH^- \quad (7)$$

This equation, called Elsner's equation, is stoichiometrically correct. However, it does not completely describe the cathodic reactions associated with the dissolution (Marsden and House, 1992).

The dissolution mechanism has been debated under both acidic and alkaline conditions. Dissolution involves an electrochemical process in which the anodic reaction is gold oxidation while the cathodic reaction is oxygen reduction. Senanayake (2008) has illustrated the gold ion diffusion through the interfaces into the solution as shown in Figure 1.

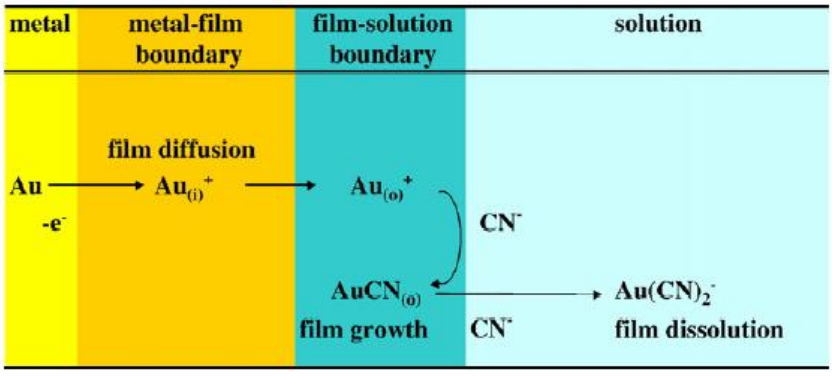

Figure 1 Anodic cyanidation model for gold; boundary i: gold-film interface, boundary o: film-solution interface (Senanayake, 2008).

The important steps during the anodic reaction in the solution phase are presented below (Kondos *et al*, 1995; Ling *et al*, 1996; Wadsworth *et al*, 2000):

(a) Adsorption of cyanide on gold surface

$$Au + CN^-(aq) \rightleftharpoons AuCN^-(s) \quad (8)$$

(b) Electrochemical extraction of an electron

$$AuCN^-(s) \rightleftharpoons AuCN(s) + e^- \quad (9)$$

(c) Combination of the adsorbed intermediate with another cyanide ion

$$AuCN(s) + CN^- \rightleftharpoons Au(CN)_2^-(aq) \quad (10)$$

where (s) refers to surface adsorbed species and AuCN is a neutral intermediate species adsorbed on the surface.

(d) Overall anodic reaction

$$Au(CN)_2^- + e^- \rightleftharpoons Au + 2CN^- \quad (11)$$

for which the Nernst equation is:

$$E_h = -0.60 + 0.118\ pCN + 0.059 \log\ (C_{Au(CN)_2^-})\ V \quad (12)$$

The anodic dissolution is accompanied by the cathodic reduction of oxygen involving several parallel and series reactions:

(d) oxygen reduction to H_2O_2

$$O_2 + 2H_2O + 2e^- \rightleftharpoons H_2O_2 \qquad E_h = 0.69\text{-}0.059\ pH\text{-}0.0295\ pO_2 \quad (13)$$

(e) hydrogen peroxide decomposition

$$2H_2O_2 \rightleftharpoons O_2 + 2H_2O \quad (14)$$

(f) oxygen reduction to hydroxide ions

$$O_2 + 2H_2O + 4e^- \rightleftharpoons 4OH^- \qquad E° = 0.401\ V \quad (15)$$

The hydrogen peroxide formed is a strong oxidizing agent which may able to reduce to hydroxide ions (OH^-) as follows:

$$H_2O_2 + 2e^- \rightleftharpoons 2OH^- \qquad E° = 0.88\ V \qquad (16)$$

However, it has been shown that the reduction of this species is difficult to happen and the dissolution rate of gold in oxygen-free solutions containing hydrogen peroxide is very slow (Marsden and House, 1992).

Figure 2 illustrates the major reactions of the two electron processes. The rate limiting conditions appear when the diffusion rates of cyanide and oxygen are equal. Then the slower diffusion rate of any species will provide the rate limiting factor (Marsden and House, 1992). The slow rate has been related to the formation of a passive layer on gold surface as well (Zheng *et al*., 1995).

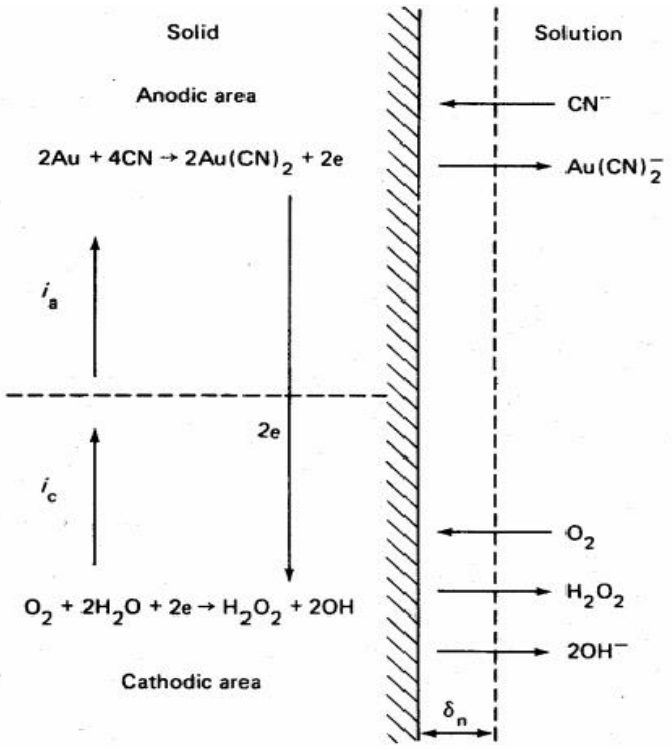

Figure 2 Schematic representation of the local corrosion cell at a gold surface in contact with an oxygen-containing cyanide solution. i_a is the anodic current; i_c is the cathodic current (Marsden and House, 1992).

2.3 Competitive Reactions in Alkaline Cyanide Solution

Many other elements and minerals are able to dissolve in dilute alkaline cyanide solution as well. These competitive reactions may increase reagents consumption and consequently reduce the efficiency of gold leaching. The sulfides, for example, are dissolved and produce metal cyanide complexes and various sulfur-containing species, such as sulfate, sulfide, thiocyanate and thiosulfate ions. For instance, pyrrhotite which is the most reactive iron sulfide in alkaline cyanide solution reacts with cyanide to form thiocyanate as presented in the following equation (Deschênes *et al*, 1998):

$$Fe_7S_8 + CN^- \rightleftharpoons 7FeS + SCN^- \quad (17)$$

and further oxidation produces Fe(II) cyanide:

$$2FeS + 12CN^- + 5O_2 + 2H_2O \rightleftharpoons 2Fe[CN]_6^{4-} + 2SO_4^{2-} + 4OH^- \quad (18)$$

The $Fe[CN]_6^{4-}$ complex is stable in the pH range used in cyanidation, as indicated in E_h-pH diagram for the Fe-S-CN-H_2O system at 25 ˚C (Marsden and House, 1992). It indicates that the ferrocyanide complex can decompose at higher pH. Iron hydroxide is the most likely precipitate after the ferrocyanide complex is completely dissociated. The reaction is given as (Rees and van Deventer, 1999):

$$2Au + \tfrac{2}{3}Fe(CN)_6^{4-} + \tfrac{1}{2}O_2 + H_2O \rightleftharpoons 2Au(CN)_2^- + 2OH^- + \tfrac{2}{3}Fe^{2+} \quad (19)$$

Other minerals, such as copper, and metal oxides are soluble to form metal cyanide complex in alkaline cyanide solutions as well. Chalcopyrite ($CuFeS_2$) is one of common copper minerals showing low solubility in cyanide solution. It is reported that concentration of this copper mineral between 300 and 400 ppm in solution does not affect gold leaching. All other common copper minerals, for example, chalcocite (Cu_2S) and cuprite (Cu_2O) have higher solubility. The possibly competitive reactions are shown below (Vukcevic, 1997):

$$Cu_2O + 5CN^- + \tfrac{1}{2}O_2 + H_2O \rightleftharpoons 2Cu(CN^-)_2^- + OCN^- + 2OH^- \quad (20)$$

$$Cu_2S + 5CN^- + \tfrac{1}{2}O_2 + H_2O \rightleftharpoons 2Cu(CN^-)_2^- + S + OCN^- + 2OH^- \qquad (21)$$

These minerals generally consume fewer amounts of cyanide and oxygen than sulfide. However, the species formed may affect precipitation reactions and overall process efficiency (Marsden and House, 1992). Consequently, several pretreatment methods, for example, pre-aeration, pressure oxidation and roasting are applied to the leach slurry prior to cyanidation in order to reduce the oxygen and cyanide consumption.

2.4 Oxidation-Reduction Potential (ORP)

Redox potential or ORP can be used to explain the stabilities of metals and other species in aqueous solutions. ORP is related to the potential-pH diagrams, also called E_h-pH or Pourbaix diagrams, by Nernst equation. Each line on the E_h-pH diagram represents the condition where the activities of reactants and products of the considered reaction are in equilibrium. Figure 3 illustrates the E_h-pH conditions applied in industrial gold extraction process. This Pourbaix diagram indicates that the reaction of the Au(I) complex takes place more readily than the Au(III) complex since the E_h value of the Au(I) complex reaction is more negative than the other. Wadsworth *et al*. (2000) presented that gold dissolution in alkaline cyanide solution ($Au(CN)_2^-$) was found to occur at the redox potential range of -0.4 and -0.7 V. Figure 3 also indicates that the potential difference between the lines of gold oxidation and oxygen reduction reactions is maximized at pH value of about 9.5. The Pourbaix diagram is also able to explain the role of other minerals competing with gold cyanidation.

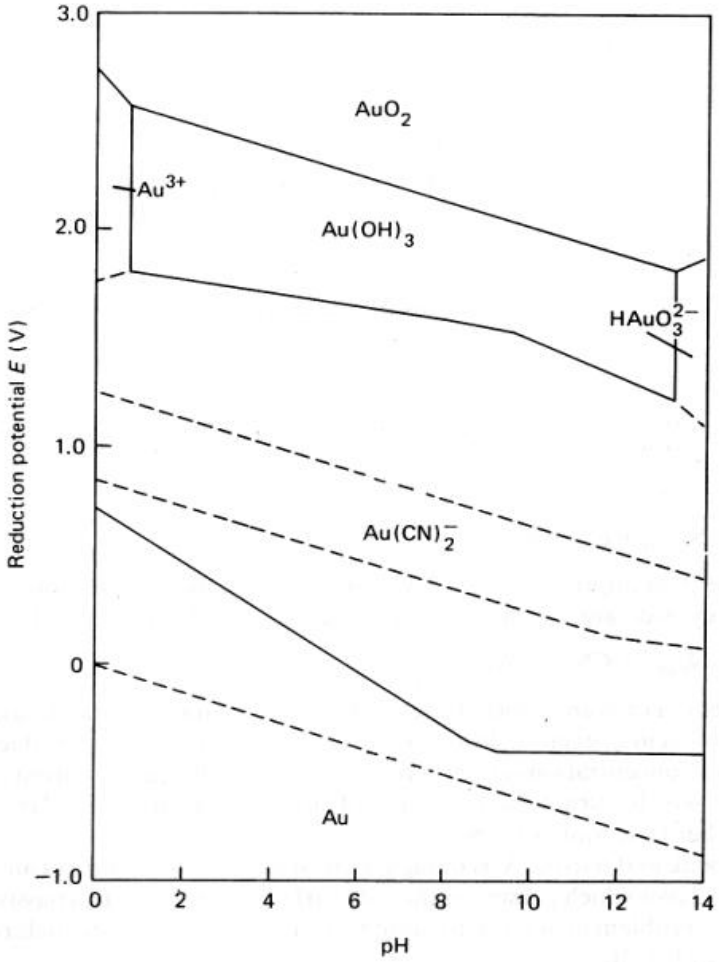

Figure 3 Potential-pH diagram for the system Au-H_2O-CN^- at 25 ºC. Concentrations of all soluble gold species = 10^{-4} M (Marsden and House, 1992).

Figure 4 illustrates the iron mineral system, one of the important competitve minerals in alkaline cyanide solution. Figure 4 shows that the iron(II) complex can be formed readily. According to the comparison between the Figures 3 and 4, it can be seen that the Fe(II) complex is more reactive in cyanide solution than Au(I) at the same value of pH since the E_h value of the Fe(II) complex is more negative. Therfore, the iron minerals might be reacted with cyanide thus retarding gold dissolution. However, the E_h value also depends on process conditions.

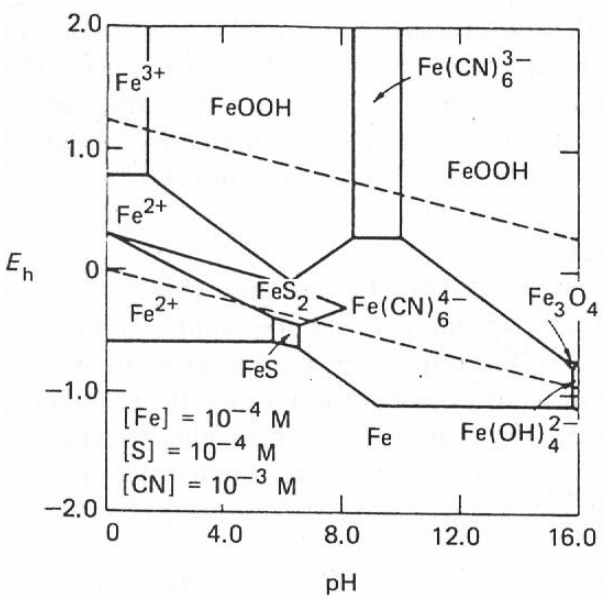

Figure 4 E_h-pH diagram for the Fe-S-CN-H_2O system at 25˚C (Marsden and House, 1992).

3 PHENOMENA IN GOLD LEACHING

The most important reactions in hydrometallurgical gold extraction processes are heterogeneous, involving the transfer of metals and minerals between solid and liquid phases. Heterogeneous reactions are controlled either by the inherent chemical reaction kinetics or by the rate of mass transfer of the individual reacting species across a phase boundary (Marsden and House, 1992).

3.1 Reaction Kinetics

Many researchers have attempted to model the kinetics of gold dissolution. The rotating gold discs have been used in fundamental studies to determine the rates at a constant surface area, assuming that the surface roughness does not change during the course of reaction. It was concluded that the rate of pure gold dissolution relies on the rate of film diffusion of cyanide ions or dissolved oxygen towards the gold surface as shown below (Kondos *et al*., 1995; Ling *et al*., 1996):

$$-\frac{dN_{Au}}{A\,dt} = \frac{2D_{CN^-}D_{O_2}C_{CN^-}C_{O_2}}{\delta\{(D_{CN^-}C_{CN^-}) + (4D_{O_2}C_{O_2})\}} \qquad \text{mol m}^{-2}\,\text{s}^{-1} \qquad (22)$$

where A surface area of gold disc in contact with aqueous phase, m^2

C_{CN^-} cyanide concentration, mol/m_L^3

C_{O_2} oxygen concentration, mol/m_L^3

D_{CN^-} diffusion coefficients of cyanide, m^2/s

D_{O_2} diffusion coefficient of oxygen, m^2/s

N_{Au} amount of gold in particles, mol

t time, s

δ The Nernst boundary layer thickness, m

From Equation (22), it can be seen easily that when $D_{CN^-} C_{CN^-} < 4D_{O_2} C_{O_2}$ or low cyanide concentration, gold dissolution rate depends primarily on that cyanide concentration:

$$-\frac{dN_{Au}}{Adt} = \frac{1}{2}\frac{D_{CN^-}}{\delta} C_{CN^-} = k_{CN^-} C_{CN^-} \qquad \text{mol m}^{-2}\,\text{s}^{-1} \qquad (23)$$

where k_{CN^-} rate constant, s^{-1}

Similarly, for high cyanide concentration, the gold dissolution rate becomes mainly dependent on the oxygen concentration:

$$-\frac{dN_{Au}}{Adt} = 2\frac{D_{O_2}}{\delta} C_{O_2} = k_{O_2} C_{O_2} \qquad \text{mol m}^{-2}\,\text{s}^{-1} \qquad (24)$$

where k_{O_2} rate constant, s^{-1}

In practice, a high level of cyanide has been maintained rather than a high dissolved oxygen level in the solution. Consequently the majority of the mills operate at cyanide levels such that gold dissolution is dependent on the dissolved oxygen level (Kondos *et al.*, 1995). However, the use of Equations (22)-(24) is limited in modeling an industrial process due to the difficulty in measuring the exact gold surface area in the ore and Nernst boundary layer thickness (Ling *et al.*, 1996).

An expression of second order rate equation was proposed by Nicol *et al.* (1984), as presented in Equation (25). This equation, the so called Mintek equation, was presented as an empirical equation based on the leaching behavior of several South African gold ores and has the following form (Ling et al., 1996; Crundwell and Gordorr, 1997):

$$-\frac{d C_{Au}}{dt} = k (C_{Au} - C_{Au}^{\infty})^2 \qquad \text{mg kg}^{-1}\,\text{s}^{-1} \qquad (25)$$

where k overall rate constant, kg/mg s

C_{Au} gold concentration in particles, mg/kg

C_{Au}^{∞} gold concentration in particles after infinite leaching time, mg/kg

This equation neither accounts for the reagent concentration, C_{CN^-} and C_{O_2}, nor for the particle size (Ling *et al*., 1996; de Andrade Lima and Hodouin, 2005). Consequently, many researchers have further endeavored to present the kinetics involved a term of the reactants.

Ling *et al*. (1996) proposed a single rate equation on the assumption of pseudo-homogeneous ore behavior. This rate equation can be expressed in terms of mass per mass of ore instead of mass per surface area of gold units, as follows:

$$-\frac{d\,C_{Au}}{dt} = k\,C_{CN^-}{}^{\alpha}\;C_{O_2}{}^{\beta}\,(C_{Au} - C_{Au}^{\infty})^{\gamma} \qquad \text{mg kg}^{-1}\,\text{h}^{-1} \qquad (26)$$

where C_{Au} gold concentration in particles, mg/kg

C_{Au}^{∞} gold concentration in particles after infinite leaching time, mg/kg

C_{CN^-} cyanide concentration, mg/dm^3

C_{O_2} oxygen concentration, mg/dm^3

k overall rate constant, unit depends on reaction orders

α reaction order for cyanide

β reaction order for oxygen

γ reaction order for gold

In the model, a reaction order of 1.5 for gold was found to be the best fit to experimental data. They also found that the overall rate constant, *k*, equals to 0.0016 ± 0.0002, α equals to 0.81 ± 0.10 and β equals to 0.73 ± 0.09 within the examined range of C_{CN^-} 25-156 mg/dm^3, C_{O_2} 8.5-40 mg/dm^3, C_{Au} 4.7-13.2 mg/kg and pH 10. This equation does not account for the ore particle size. However, it was claimed to be used for preliminary process analysis.

de Andrade Lima and Hodouin (2005) has recently developed the rates equation describing the gold dissolution, using the general pseudo-homogeneous kinetic equation, as presented in equation (26), considering also the particle size. The overall rate constant, *k*, is a function of the average diameter of the ore particles, as follows:

$$k = c_1 - c_2\,\bar{d}^{\,\theta} \tag{27}$$

where c_1, c_2 coefficients, units depend on reaction order

$\bar{d}$ average diameter of particles, μm

θ exponent for average diameter of ore particles

The gold dissolution kinetic equation shows that the reaction orders are approximately two for gold, one for free cyanide and a quarter for dissolved oxygen. The constant is a decreasing cubic function of the average particle diameter and may be controlled by the particle volume. The rate equation for gold dissolution is shown below:

$$-\frac{d\,C_{Au,c}}{dt} = (1.13\times10^{-3} - 4.37\times10^{-11}\,\bar{d}^{\,2.93})\times\,(C_{Au,c} - C_{Au,c}^{\infty})^{2.13} \times C_{CN^-}{}^{0.961}\; C_{O_2}{}^{0.228} \qquad \text{mg kg}^{-1}\,\text{h}^{-1} \tag{28}$$

This equation was obtained by using free cyanide concentrations 260 and 650 mg/dm^3, dissolved oxygen concentrations 8 and 40 mg/dm^3, gold content in the ore 1.5-2.3 mg/kg and pH 12. This equation was proved to fit well the fine size fractions because gold particle segregation was negligible and small samples could adequately represent the system, while this is acceptable for the coarse particles. Since cyanide is not a selective leaching agent, it can react with other chemical species, such as zinc, iron, silver and copper minerals. Thus, de Andrade Lima and Hodouin (2005) also investigated the kinetic model for the cyanide consumption as a function of cyanide concentration and particle size. The following pseudo-homogeneous model describes the consumption process:

$$-r_{CN^-} = k_{CN^-} C_{CN^-}{}^{\eta} \qquad \text{mg dm}^{-3}\ \text{h}^{-1} \qquad (29)$$

$$k_{CN^-} = \frac{c_3}{\bar{d}^{\theta} - c_4} \qquad (30)$$

where C_{CN^-} cyanide concentration, mg/dm^3

c_3, c_4 coefficients, units depend on reaction order

$\bar{d}$ average diameter of particles, μm

k_{CN^-} overall rate constant which is a function of the average diameter of particle, (dm^3/mg)$^{2.71}$ h^{-1}

θ exponent for average diameter of ore particles

The estimated cyanide consumption kinetic shows that the reaction order is approximately three for free cyanide. The rate constant is a decreasing reciprocal square-root function of the particle diameter. The free cyanidation model is then given as follows:

$$-r_{CN^-} = \left(\frac{1.69 \times 10^{-8}}{\bar{d}^{0.547} - 6.40} \right) C_{CN^-}{}^{3.71} \qquad \text{mg dm}^{-3}\ \text{h}^{-1} \qquad (31)$$

It was also found that the cyanide consumption kinetics are faster for the small particles due to the liberation of the cyanide-consuming species found in the ore (de Andrade Lima and Hodouin, 2005).

The electrochemical reaction mechanism was also used to describe the rate of gold leaching by Crundwell and Godorr (1997) as given below:

$$-\frac{d N_{Au}}{A dt} = \frac{1}{F} (k_a C_{CN^-})^{0.5} (k_c C_{O_2})^{0.5} \qquad \text{mol m}^{-2}\ \text{s}^{-1} \qquad (32)$$

where F the Faraday constant, 96,485.34 C/mol

k_a rate constant of anodic half-reaction, C m/mol s

k_c rate constant of cathodic half-reaction, C m/mol s

The rate expression which is derived from the anodic and cathodic half-reactions is one-half order in the concentrations of cyanide and oxygen. The cyanide concentration determines the rate of anodic dissolution of gold while the oxygen concentration determines the cathodic reduction of oxygen (Crundwell and Godorr, 1997).

3.2 Gas-Liquid Mass Transfer

Mass transfer from gas to liquid phase has a significant role in cyanidation using oxygen in the stirred tank reactor. Gas is introduced in the form of bubbles into the liquid by an appropriate distributor. The gas-liquid mass transfer is normally described by the volumetric mass transfer coefficient, k_La s^{-1} where k_L is the mass transfer coefficient, m/s, and a is the specific interfacial area, m^2/m^3. The most important characteristics affecting the gas-liquid mass transfer are the energy dissipation, the gas hold-up and the bubble size. These variables are a function of the vessel geometry, mainly the stirrer and gas distributor, and operational conditions such as power input and gas flow. Physical properties of solution and gas phase, for example, viscosity, surface tension and density also have effect on the parameters of gas-liquid mass transfer (Garcia-Ochoa and Gomez, 2004).

Researchers have attempted to present the volumetric mass transfer coefficient by using the experimental data and empirical correlations obtained in stirred tank reactor. Garcia-Ochoa and Gomez (2004) have presented a correlation for the k_La as follows:

$$k_La = mU_G^x(P/V)^y\mu^z \quad s^{-1} \quad (33)$$

where m constant

P power input under gassed conditions, W

U_G superficial gas velocity, m/s

V volume of liquid in vessel, m^3

μ viscosity, Pa s

Other equations proposed substitute the average power input per volume, P/V, by the effect of stirrer speed, N. Garcia-Ochoa and Gomez (2004) also have presented the volumetric mass transfer coefficient for different stirred tank volumes and for both Newtonian liquid, which is air-water system, and non-Newtonian liquid, such as air-sodium sulfite solution system. The exponents (x, y and z) are shown in many different dimensional correlations based on tank configurations, properties of liquid and operational conditions as given in Table 1.

The stirred tanks presented are single and multi impeller systems such as flat blade turbine, flat blade paddle, pitched blade paddle and two stirrers of flat blade turbine with four blades. Garcia-Ochoa and Gomez (2004) have found an increase in k_La with the increasing of superficial gas velocity, power input (stirred speed) and liquid viscosity. Fan and Herz (2007) have proposed that the k_La values between 0.05-0.5 s^{-1} can be achieved in most well-designed stirred tank reactors. They have found that the k_La value for CO_2-Na_2CO_3 solution system was 0.06 s^{-1}, where the k_L and a values were 7.2 $\times 10^{-4}$ m/s and 84 m^2/m^3, respectively. Lorenzen and Kleingeld (2000) have presented the k_La value for carbon dioxide gas-sodium hydroxide (CO_2-NaOH) solution system in the high intensity gas-liquid jet reactor. The results have been shown to exhibit high mass transfer coefficient, interfacial areas and volumetric mass transfer coefficient compared to the conventional system. The k_L value was up to 3×10^{-3} m/s while the value of a was ranging from 2000 to 16000 m^2/m^3. Consequently, the k_La was up to 25 s^{-1} which is higher than the k_La for conventional processes in the region of 0.025-1.25 s^{-1}. Lorenzen and Kleingeld (2000) have claimed that these results can be compared to the possibly enhanced mass transfer rates when using oxygen or air during cyanidation.

Table 1 Exponent values (*x*, *y*, *z*) for each variable in the dimensional correlations for k_La proposed by different authors (Garcia-Ochoa and Gomez, 2004).

System	**Authors**	N (s^{-1})	$(U_G)^x$ (m/s)	$(P/V)^y$ (W/dm^3)	$(\mu_a)^z$ (Pa s)	**Volume** (dm^3)	**Stirrer type**
Newtonian	Yagi and Yoshida		0.3	0.8		12	6FBT
	Figueirado and Caiderbank		0.8	0.6		600	FBT
	Van't Riet		0.5	0.4		2-2600	Any
	Nishikawa *et al.*	2.4	0.33	0.8		2.65-170	FBT and FBP
	Davies *et al.*		0.45	0.8		20-180	6FBT
	Linek *et al.*		0.4	0.65		20	6FBT
	Gagnon *et al.*		0.5	0.6-0.8		22	6FBT
	Arjunwadka *et al.*		0.58	0.68		5	FBT and PBT
	Vasconcelos *et al.*		0.49	0.62		5	Two-6FBT
Non-Newtonian	Yagi and Yoshida	2.2	0.3		-0.4	2.65	FBT and FBP
	Nishikawa *et al.*	2.4	0.3	0.8	-0.5	2.7-170	FBT and FBP
	Linek *et al.*		0.4	1.1		20	6FBT
	Pedersen *et al.*	2.7	0.5-0.7			15	Two-6FBT
	Arjunwadkar *et al.*		0.4	0.68		5	FBT and PBT
	Garcia-Ochoa and Gomez	2.0	0.5		-0.67	2-25	FBT,CBT,CBP

3.3 Solid-Liquid Mass Transfer

Solid-liquid dispersion in mechanically agitated vessels or stirred tank reactors has been widely studied. The main reason for applying the mechanical agitation is to ensure that all of the surface area available for mass transfer is utilized. Evaluation of the solid-liquid mass transfer coefficient, k_{SL}, has often been performed by solid dissolution. This coefficient is dependent upon the homogeneity, which is the function of geometric configurations (type of impeller, impeller size to tank size ratio or d_D/d_T, impeller location or X/d_T), operating parameters (impeller speed, power input, particle loading) and physical properties of the particles and fluid (viscosity, solid-liquid density difference, particle size and shape). The turbulence intensity close to the impeller is the highest and decreases as the distance from the impeller increases (Pangarkar *et al.*, 2002).

Pangarkar *et al.* (2002) have presented a correlation for the solid-liquid mass transfer coefficient in three-phase (solid-liquid-gas) system, where the type and the location of the sparger and gas flow rate are taken into account. The correlations are presented on the basis of classified approaches which are dimensional analysis, Kolmogoroff's theory of isotropic turbulence, slip velocity theory and analogy between momentum transfer and mass transfer. The dimensional approach-based correlations are presented in terms of Sherwood number based on tank diameter, Sh_T ($k_{SL}\,d_T/D_m$), and particle diameter, Sh_P ($k_{SL}d_P/D_m$). The correlations are given in Table 2. Pangarkar *et al.* (2002) suggested a correlation with many variables such as liquid viscosity and density, impeller speed, d_D/d_T and particle size. Some correlations are presented only on the terms of Reynolds number based on impeller diameter, Re_N ($Nd_D^2\rho/\mu$) and tank diameter, Re_T ($Nd_T^2\rho/\mu$) and Schmidt number, Sc ($\mu/\rho D_m$), while some have several variables. The constants and the exponent of the Reynolds number and Schmidt number vary with geometric configurations and operating parameters. Thus, the application of the correlation based on dimensional approach is limited since it predicts widely different k_{SL} values and can only be applied to geometrically similar configuration under similar range of operating parameters. The estimation of k_{SL} values from momentum transfer-mass transfer

approach-based correlations, which correlate relative particle suspension, is claimed to be reliable and simple. In this case, k_{SL} is a function of impeller speed and Schmidt number. Other approaches, to correlate k_{SL}, are also presented as a function of Reynolds number and Schmidt number with different exponent values. However, there are also limitations in the Kolmogoroff's theory about geometric variables and in the density difference and slip velocity theory about turbulence characteristics (Pangarkar *et al*., 2002).

In the case of fine particles ($d_P \leq 100$ μm), which are commonly found in processes such as crushed ores in leaching tank, the mass transfer coefficient increases greatly with decreasing particle size. The k_{SL} values are claimed to be independent of the density difference and tank diameter and can be correlated as $Sh_P = f(Re_\varepsilon, Sc)$ based on the Kolmogoroff's theory. In the correlation, the Sherwood number based on the particle diameter, Sh_P, is a function the Reynolds number and Schmidt number (Pangarkar *et al*., 2002).

Table 2 Correlations based on dimensional approach proposed by different authors (Pangarkar *et al*., 2002).

Investigators[a]	Correlation proposed
Hixon and Wilkens (UB)	$(k_{SL}\ d_T)/(So\ D_m) = f(Nd_T{}^2\rho_L/\mu)$
Hixon and Baum (UB)	for turbine, $Sh_T = 2.7\times10^{-5}\ (Re_T)^{1.4}(Sc)^{0.5}$; $Re_T < 6.7\times10^4$; $Sh_T\ 0.16(Re_T)^{0.62}(Sc)^{0.5}$; $Re_T > 6.7\times10^4$; for marine propeller, $Sh_T = 3.5 \times 10^{-4}(Re_T)^{1.0}(Sc)^{0.5}$
Mack and Marriner (B)	$(Sc)^q(Sh_T)(H/d_T)^{0.15} = f(N_{Po}, Re_N)$
Humphrey and VanNess (B)	for turbine, $Sh_T = 0.0032(Re_T)^{0.87}(Sc)^{0.5}$; for propeller, $Sh_T = 0.13(Re_T)^{0.58}(Sc)^{0.5}$
Kolar (B)	$Sh_T = 0.0399(Re_T)^{0.67}(Sc)^{0.5}$
Nagata *et al*. (B,UB)	$Sh_T = \text{const}(Re_T)^p(Sc)^{0.5}(d_P/d_T)^q$, $0.20 < p < 0.67$; $-0.8 < q < -0.32$
Barker and Treybal (B)	$Sh_T = 0.02(Re_N)^{0.833}(Sc)^{0.5}$
Marangozis and Johnson (B, UB)	for baffled vessel, $Sh_T = 0.402(Re_N)^{0.65}(Sc)^{0.33}$; $500 < Re_N < 60\ 000$; for unbaffled vessel, $Sh_T = 0.635(Re_N)^{0.70}(Sc)^{0.33}$; $100 < Re_N < 100\ 000$
Sykes and Gomezplata (B)	$Sh_P = 2+0.109[(Re_N i)(N_{Poi}/N_{PoFDT})]^{0.38}(Sc)^{0.5}$
Jha and Raja Rao (UB)	for baffle vessel, $Sh_T = 0.52(Re_N)^{0.66}(Sc)^{0.33}(X/d_T)^{-0.20}$ for unbaffled vessel, $Sh_T = 0.27(Re_N)^{0.83}(Sc)^{0.33}$
Nagata (B,UB)	$Sh_T = 3.60\times10^{-2}\ (Re_T)^P(Sc)^q(D_m2/d_T{}^2g)^{0.627}(d_P/d_T)^{3.08}(\Delta\rho/\rho_L)^{-2.82}$; here, $P = f(g, d_T, \upsilon, \Delta\rho/\rho_L)$ and $q = f(d_P/d_T, \Delta\rho/\rho_L)$
Blasinski and Pyc (B,UB)	for baffled vessel, $Sh_T = 0.60\times10^{-2}\ (Re_T)(Sc)^{0.5}(d_D/d_T)(\rho_S/\rho_L)^{0.25}$fr; for unbaffled vessel, $Sh_T = 0.115\ (Re_T)^{0.6}(Sc)^{0.5}(d_D/d_T)^{0.75}(\rho_S/\rho_L)^{2.25}\ (u_A)^K(d_P/d_D)^{-0.33}$fr; here fr is reaction factor; $K = f(c)$
Boon-Long *et al*. (B)	$Sh_P = 0.046(Re_p)^{0.283}(Ga)^{0.173}(m_T/\rho_L d_P{}^3)(d_T/d_P)^{0.019}(\upsilon/D_m)^{0.461}$

[a] Term in bracket next to investigator's name represents type of the tank used by respective workers: (B) baffled tank; (UB) unbaffled tank.

4 VARIABLES AFFECTING THE PHENOMENA

Leaching parameters have been widely studied to optimize the performance of the cyanidation process. Performance of process depends on variables such as the concentrations of dissolved oxygen, free cyanide and compounds that react with cyanide, pH, particle size and operating conditions. These parameters affect on the gold dissolution rate, gold extraction and cyanide consumption. Many studies have been carried out under different experimental conditions in order to investigate the effect of leaching parameters and obtain the optimum process conditions. Some of those are listed below.

Deschênes and Wallingford (1995) experimented with a sulfide bearing gold ore containing 6.75 g/t Au. The ore was grinded to the size of 74 μm. The stirring speed was kept constant at 400 min^{-1}. The ore was pre-leached with air for four hours followed by cyanidation. 95.8% Gold recovery was obtained under condition of free cyanide concentration 480 ppm, lead nitrate 200 g/t, pH 10.5 and 16 ppm O_2. The cyanide consumption in 24 hours was 0.51 kg/t

Ling *et al.* (1996) presented that the maximum gold dissolution achieved was about 93 % under ambient temperature 20 ˚C and air sparging at pH 11, dissolved oxygen of 8.5 ppm and cyanide concentration of 104 ppm. The agitation speed was maintained at 750 min^{-1} for 24 hours. Ore sample in this case was from a northern Ontario mining site and had a mean size of 37 μm.

Deschênes *et al*. (2003) performed experiments with the dissolved oxygen concentration at 10 ppm and pH at 11.2. A sample of high grade ore 77.8 g/t received from Goldcorp Red Lake Mine, Canada was milled to the size of 37 μm. The cyanide consumption for a 24-h leach was 0.55 kg/t using 300 ppm NaCN. The experiment was carried out at a constant rate of 400 min^{-1}. It was found that adding 100 grams of lead nitrate per ton to the pre-leach circuit increases gold recovery. At these conditions, about 96% gold extraction was achieved.

Ellis and Senanayake (2004) investigated gold leaching in multi-mix system at ambient temperature, pH about 10, NaCN about 200 mg/dm^3 and dissolved oxygen about 20 mg/dm^3. In this study, a pyrrhotite-rich ore, 63 μm, from the Bounty Gold mine located in Western Australia was used. They concluded that pre-oxidation for 12 h followed by cyanidation of C_{CN^-} / C_{O_2} molar ratio at about 12 provided the best gold extraction in the first cyanidation tank. The percentage of Au extracted in the first tank reached a maximum of 83% when the product $C_{CN^-} \times C_{O_2}$ was about 5.6 mmol^2/(dm^3)^2.

Consolidated Murchison located in South Africa is one of the gold industries using cyanide leaching together with oxygen. In the process, the ore is crushed to the size of about 75 μm. Around 1983, 77% gold recovery was achieved under conditions at pH 7 by lime, 2% NaCN, 52% solids and ambient temperature of 22-38˚C. Leaching is performed in a pipe reactor at a pressure of 9 MPa, with pure oxygen injected into the reactor at 12 MPa. The reactor provided a retention time of 15 min. Cyanide and oxygen consumptions were 57 and 20 kg/t, respectively (Marsden and House, 1992).

Table 3 summarizes the optimum operating conditions from various experiments as written above.

Table 3 Summary of the optimum operating conditions in some gold cyanidation studies.

Researcher	**Particle size (µm)**	**C_{CN^-} (ppm)**	**C_{O2} (ppm)**	**pH**	**Temperature (°C)**	**Stirring speed (rpm)**	**% Au Extraction**
Deschênes & Wallingford	74	480	16	10.5	-	400	95.8%with $PbNO_3 + O_2$
Ling *et al*.	37	104	8.5	11	20	750	93 % with air
Deschênes *et al*.	37	300	10	11.2	-	300	96% with $PbNO_3 + O_2$
Ellis & Senanayake	63	200	20	~10	~25	-	83% (1^{st} tank) with O_2
Consolidated Murchison	75	20 000	~150 000	7	22-38	-	77 % with O_2

4.1 Concentration of Oxygen

Oxygen is one of the key reagents in conventional gold cyanidation as presented in Equation (7). The concentration of oxygen determines the cathodic reduction of oxygen. It may be supplied to the system by air, pure oxygen or as enriched air. The oxygen concentration for processes using air is determined by the conditions of temperature and pressure that the process operates under. The saturated dissolved oxygen concentration is about 8.2 mg/dm^3 at 25˚C (Marsden and House, 1992). Ellis and Senanayake (2004) have suggested that oxygen injection, instead of air, provides a high oxygen concentration in gas to increase the oxygen solubility and can achieve high overall gold extraction. However, Kondos *et al.* (1995) found that the oxygen consumption is markedly higher with the use of oxygen gas than air. A large number of small oxygen bubbles dispersed in the slurry long enough and deep enough gives adequate oxygen concentration for gold dissolution (Ellis and Senanayake, 2004). Knowing the oxygen demand the process can be optimized in order to obtain higher gold recovery, shorter retention time, low cyanide consumption which reduces environmental concerns relating to cyanide in the effluents. However, different mineralogical compositions need different amount of oxygen, for example, pyrite-rich ore has a higher oxygen demand than ore containing albite, quartz and chlorite as the main minerals (Kondos *et al*., 1995).

Many researchers have concluded that increasing the dissolved oxygen concentration increases the rate of dissolution (Marsden and house, 1992; Deschênes *et al*., 2003; Ellis and Senanayake, 2004). Deschênes *et al*. (2003) have presented the effect of dissolved oxygen on gold extraction as illustrated in Figure 5. They discussed that dissolved oxygen concentration has no significant effect on cyanide consumption and further discussed that faster leaching kinetics were observed by using higher dissolved oxygen concentrations.

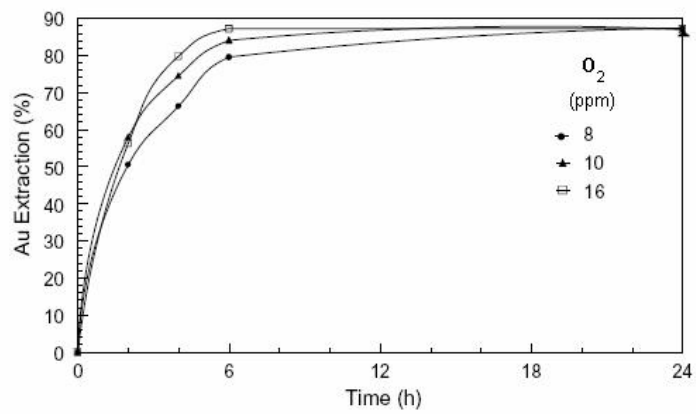

Figure 5 Effect of oxygen addition on cyanidation: pH 11.2, 500 ppm NaCN, 24 h (Deschênes *et al.*, 2003).

However, Ling *et al.* (1996) have presented Figure 6 and concluded that high dissolved oxygen level did not have significant effect on gold dissolution rate at the cyanide concentration level of 104 ppm.

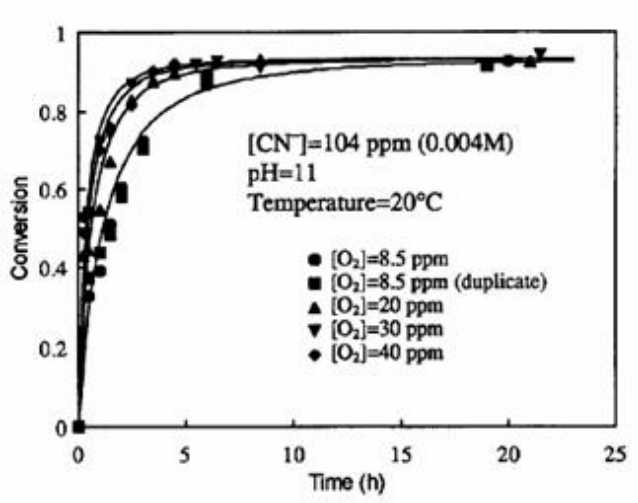

Figure 6 Effect of dissolved oxygen concentration on gold conversion (Ling *et al.*, 1996).

4.1.1 Solubility of Oxygen

The oxygen solubility depends on many factors such as temperature, pressure and ionic strength (Ellis and Senanayake, 2004). Ling *et al.* (1996) have discussed that the oxygen level in the solution is mainly affected by temperature and pressure. The solubility of gases in aqueous solutions generally increases with decreasing

temperature and increasing gas partial pressure. The ionic strength is relative low and its effect on gas solubility is not important (Ling *et al.*, 1996).

4.2 Cyanide Concentration

Many studies have presented that gold extraction increases with increasing cyanide concentration (Marsden and House, 1992; Kondos *et al*., 1995; Ling *et al*., 1996; Wadsworth *et al*., 2000; Deschênes *et al*., 2003). Figure 7 shows the effect of cyanide concentration on gold conversion.

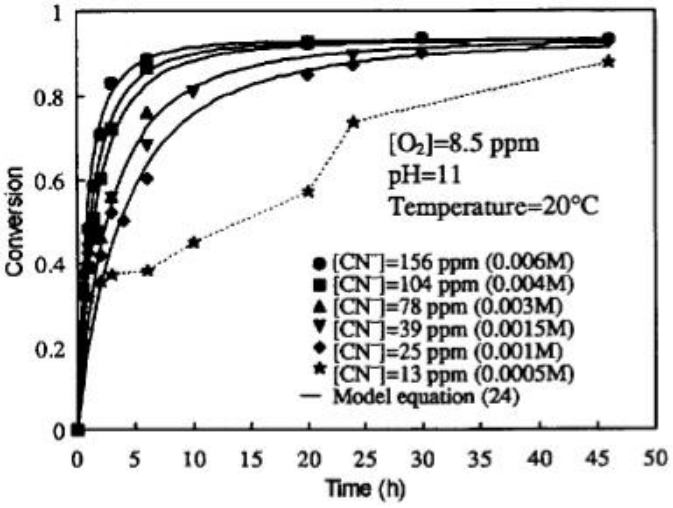

Figure 7 Effect of cyanide concentration on gold conversion (Ling *et al*., 1996).

Ling *et al.* (1996) have found that the gold dissolution rate was not very sensitive to the change of cyanide concentration at high cyanide levels. This was also found by Deschênes *et al*. (2003) who presented in Figure 8 that the use of 400-500 ppm NaCN resulted in similar overall gold extraction.

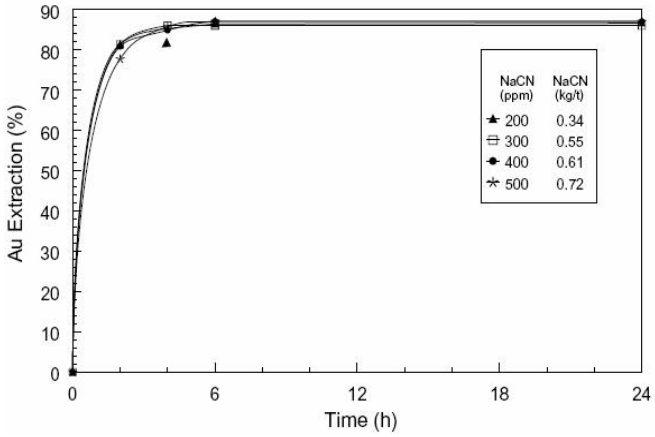

Figure 8 Effect of cyanide concentration on leaching. Pre-leaching: pH 11.2, 8 ppm O_2, 100 g/t $Pb(NO_3)_2$, 12 h; cyanide: pH 11.2, 10 ppm O_2 (Deschênes *et al.*, 2003).

Ellis and Senanayake (2004) have proposed that the rate of gold leaching increases with increasing concentration of cyanide but becomes independent of cyanide concentration when it exceeds 0.075% KCN (or 0.06% NaCN, equivalent to 600 ppm). Kondos *et al.* (1995) have concluded that using an excess of cyanide results in unnecessary cyanide consumption and has no beneficial effect on gold extraction. The excess cyanide will consume more cyanide because of the formation of cyanocomplexes from impurities. However, a high concentration of cyanide may be required due to the competition of other species such as ore containing soluble sulfides (Mardens and House, 1992). Furthermore, the decrease in cyanide concentration decreases cyanide consumption as well. The use of lower cyanide level can reduce the effluent treatment cost at the plant scale (Ling *et al.*, 1996; Deschênes *et al.*, 2003). Therefore, lower or higher cyanide concentrations than the optimum value can provide negative consequence to the gold leaching process.

4.3 pH

The addition of lime (CaO) is typically used to maintain pH in gold leaching circuit (Ling *et al.*, 1996; Ellis and Senanayake, 2004). The gold dissolution rate is expected to reduce with increasing pH since the adsorption of OH^- ion onto gold surface decreases the surface available for cyanide leaching (Kondos *et al.*, 1995;

Ling *et al*., 1996). This is also due to an increase in the rate of competing reactions such as dissolution of sulfides and other reactive species (Marsden and House, 1992). Parga *et al.* (2007) have presented the effect of pH on gold extraction as given in Figure 9. It can be seen that the gold extraction for high pressure system is reduced when pH increases as well (Parga *et al.*, 2007).

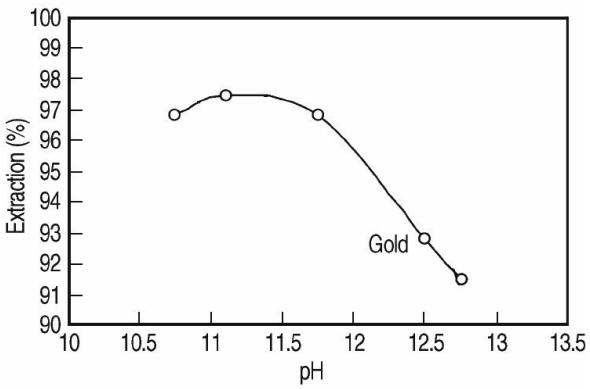

Figure 9 The effect of pH on gold extraction. Condition: 20% solid, 0.6 MPa, 300 min^{-1}, 80˚C, 1% NaCN, 1 h (Parga *et al.*, 2007).

Ellis and Senanayake (2004) have reported that cyanide leaching at high pH is able to minimize the formation of hydrogen cyanide causing cyanide loss as HCN gas as presented in Equations (2)-(4). A high pH level also results in lower cyanide consumption as presented in Figure 10 (Ling *et al*., 1996). However, the optimum pH for leaching should be derived independently for each ore type and leaching system (Marsden and House, 1992).

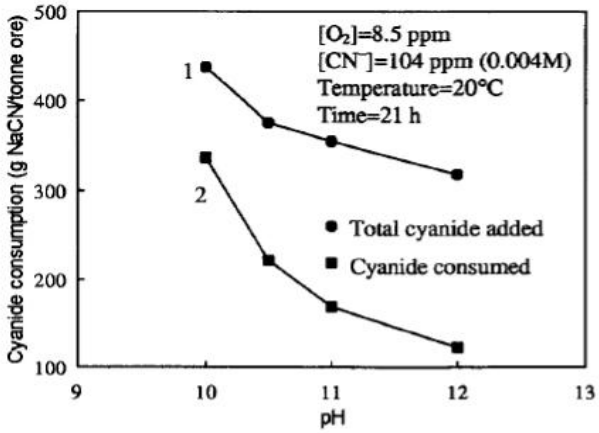

Figure 10 Effect of pH on cyanide consumption (Ling *et al*., 1996).

4.4 Particle Size

Ling *et al*. (1996) have studied the effect of particle size on gold conversion and found that smaller particle size can improve gold dissolution rate. This is because smaller particle size provides larger contacting surface area between solid and liquid and thus increases the rate. Similar results have been obtained by de Andrade Lima and Hodouin (2005) who presented the residual gold concentration in ore particle as a function of the ore particle size, as shown in Figure 11.

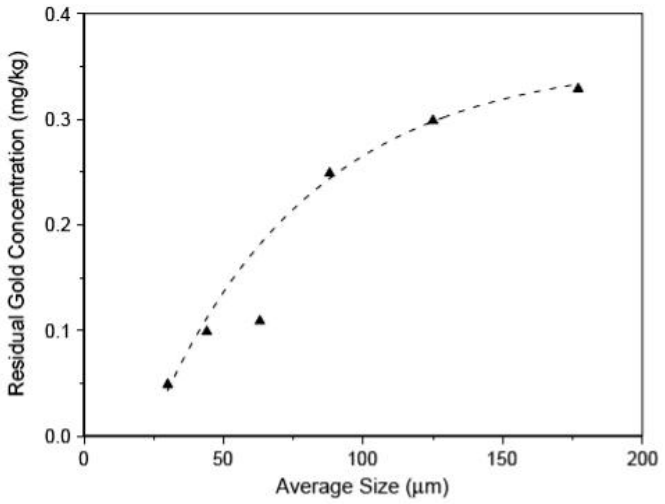

Figure 11 The residual gold concentration as a function of the ore particle size (de Andrade Lima and Hodouin, 2005).

de Andrade Lima and Hodouin (2005) have further presented the gold dissolution rate for different ore particle sizes, as displayed in Figure 12. However, Kondos *et al*. (1995) reported that increasing the fraction of finer grinding will also increase cyanide consumption and does not improve gold extraction, probably because residual gold is present in fine occlusions or in solid solution in the mineral matrix. Marsden and House (1992) also presented that the rate of dissolution may decrease with decreasing particle size due to the increased rate of competing and reagent-consuming side reactions. Moreover, the grinding costs also increase with the decrease in particle size (Ellis and Senanayake, 2004).

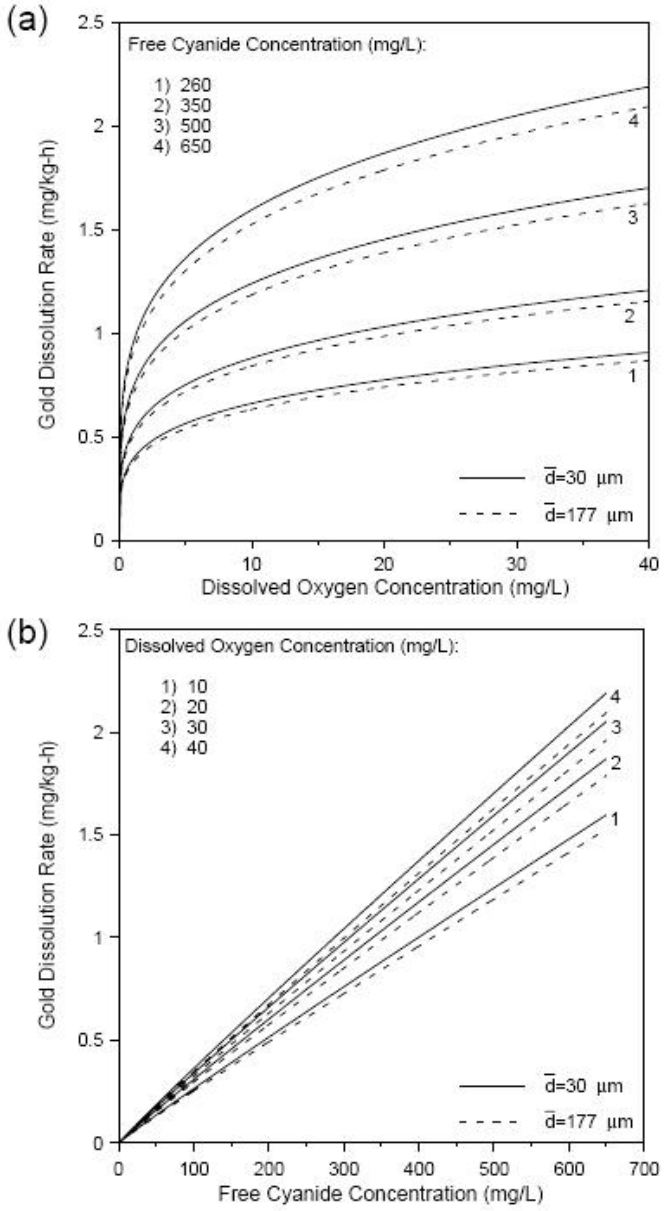

Figure 12 Gold dissolution rate for ore average particle size 30 and 177 µm: (a) as a function of the dissolved oxygen concentration; (b) as a function of the free cyanide concentration (de Andrade Lima, 2005).

4.5 Temperature

Temperature has a significant effect on gold dissolution rate and oxygen solubility. Higher temperatures result in higher reaction rates of the metals in the solvent. The viscosity of liquid is lower and the diffusivities larger at higher temperature. The gold dissolution is, therefore, aimed to increase with increasing temperature as present in Figure 13 by Marsden and House (1992). Figure 13 indicates that the

dissolution rate of gold in cyanide solution reaches maximum at approximately 85ºC. In contrast, the gas solubility tends to decrease with increasing temperature. Furthermore, temperature which is too high leads to leaching of excessive undesirable minerals as well. Consequently, the ambient temperature is usually applied (Marsden and House, 1992). However, elevated temperatures can be applied with high pressure in order to improve gold extraction as discussed in Chapter 5.3.

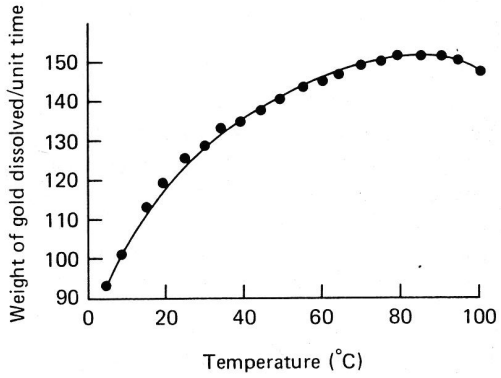

Figure 13 Effect of temperature on gold dissolution rate in aerated 0.25% KCN solution (Marsden and House, 1992).

4.6 Pressure

Pressure can improve gold dissolution in terms of gas solubility. Increasing pressure increases the solubility of gas (Ling *et al*., 1996; Ellis and Senanayake, 2004). High pressure, together with high temperature, is claimed to improve gold extraction as discussed in Chapter 5.3.

4.7 Slurry Density

Leaching is normally performed at slurry densities between 35% and 50% of solids. This is dependent upon such factors as the specific gravity of solids, particle size and the presence of minerals affecting slurry viscosity, such as clays. Mass transfer phenomena are maximized when slurry density is low. However, an increase in slurry density can increase the solids retention time in the reactor.

Furthermore, the high slurry density can reduce the reagent consumption since the slurry concentration can be obtained by smaller volume of solution per unit mass of material (Marsden and House, 1992).

4.8 Mixing

Agitation is one of the important factors in gold leaching since gold dissolution rate depends on the diffusion layer thickness and mixing characteristics of the bulk solution (Marsden and House, 1992). Therefore, agitation should be sufficient to suspend all the particles in the slurry. Increasing the agitation speed can enhance the dissolution rate since the intense mixing reduces diffusion layer thickness thus substantially improves the mass transfer rates of cyanide and oxygen and allows possible saturation of slurry with oxygen to achieve high dissolved oxygen levels (Ellis and Senanayake, 2004). Figure 14 presents the effect of impeller speed on the dissolution rate of gold disc at different oxygen concentrations.

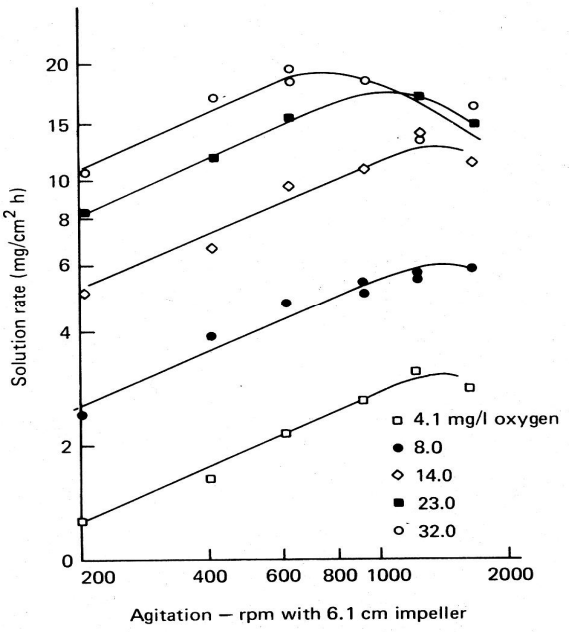

Figure 14 Effect of agitation on the dissolution rate of gold disc (Marsden and House, 1992).

4.9 Presence of Sulfide minerals and Other Ions in Solution

Many metals and minerals have a retarding effect on gold leaching rates. These metals and minerals are also able to dissolve in alkaline cyanide solution and consequently consume cyanide and oxygen. However, it was found that some ions can enhance the gold dissolution rate (Marsden and House, 1992; Aghamirian and Yen, 2005; Liu and Yen, 1995).

4.9.1 Effect of Sulfide Minerals

A sulfide mineral contains sulfide (S^{2-}) as the main anion. Most metal sulfides decompose readily in aerated alkaline cyanide solution. Sulfide minerals are also oxidized to form thiocyanate or to react with oxygen, forming sulfide and sulfate (Marsden and House, 1992). Sulfide ions are strongly adsorbed onto gold surfaces forming gold sulfide film which passivates the gold surface, and hence retards gold dissolution (Kondos *et al*., 1995) However, concerning the effect of sulfide minerals on gold dissolution, it has been found that it is dependent upon mineral types and oxygen levels in the solution (Liu and Yen, 1994).

4.9.1.1 Effect of Pyrite, Chalcopyrite and Pyrrhotite

Pyrite (FeS_2) and Pyrrhotite ($Fe_{(1-x)}S$) can introduce various sulfur species and ferrous cyanide ions into the solution, while chalcopyrite forms various cuprous cyanide compounds (Aghamirian and Yen, 2005). It has been concluded by many researchers that sulfide ions have negative effect on gold dissolution causing the surface of gold to be passivated (Marsden and House, 1992; Liu and Yen, 1994; Aghamirian and Yen, 2005; Dai and Jeffrey, 2006). The effects of sulfide minerals on gold dissolution are present in Figure 15.

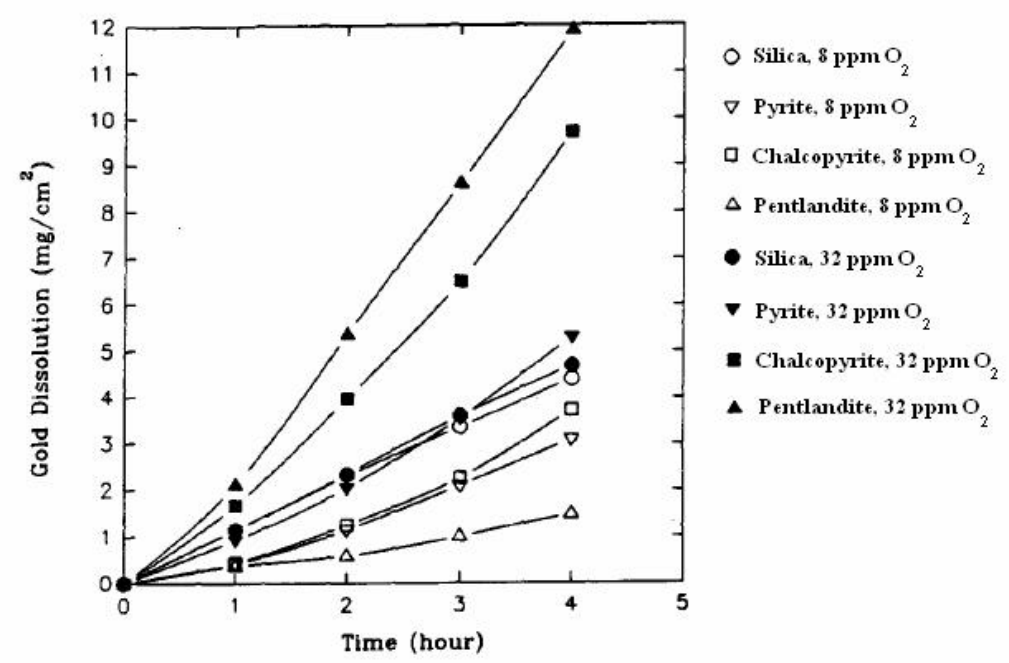

Figure 15 Effect of pyrite, chalcopyrite, pentlandite and oxygen on gold dissolution. Condition: 0.25 g of NaCN/l, 400 min^{-1}, pH 10.5, 22ºC (Liu and Yen, 1994).

Liu and Yen (1994) have concluded that gold dissolution rate is accelerated when oxygen concentration is increased in the presence of chalcopyrite and pyrite.

4.9.1.2 Effect of Galena and Arsenopyrite

The effect of galena (PbS) on gold dissolution rate is quite different from those sulfide minerals discussed earlier. The addition of galena causes the gold dissolution to be increased under atmospheric condition at 8 ppm O_2. This is because a small amount of metal ions is dissolved. The positive effect is also found in Arsenopyrite (FeAsS). Contrastingly, the gold dissolution rate reduces under oxygen-enriched condition, 20 ppm O_2, where large amounts of galena and arsenopyrite are dissolved. The rate of gold dissolution is, therefore, reduced. The rate is found to be almost zero in galena slurry at 32 ppm O_2 (Liu and Yen, 1994). Figure 16 illustrates the effect of galena and arsenopyrite on gold dissolution.

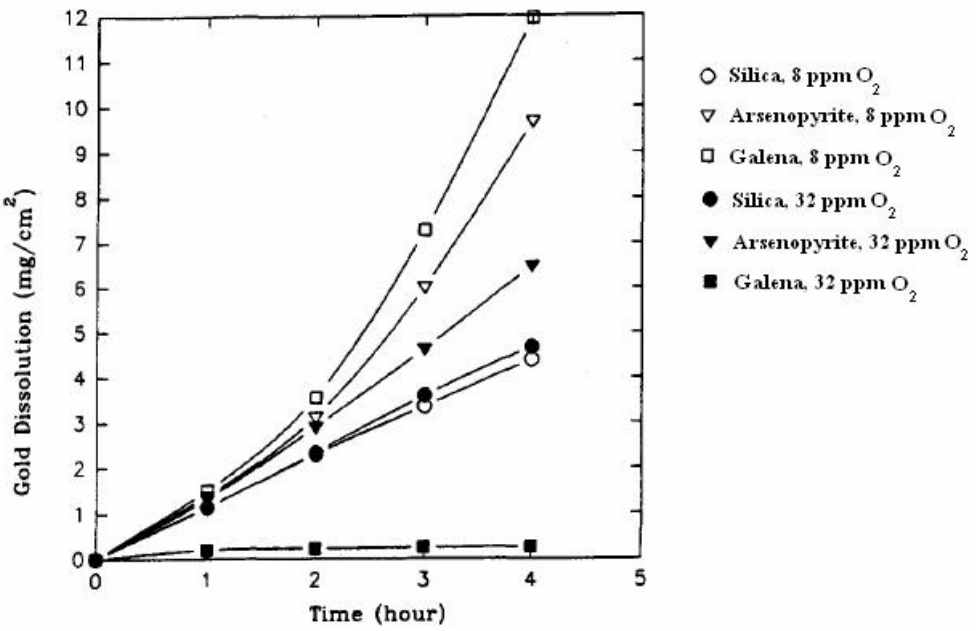

Figure 16 Effect of arsenopyrite, galena and oxygen on gold dissolution (Liu and Yen, 1994).

It might be concluded that the accelerating and retarding effects of sulfide minerals are associated with the solubility of minerals in cyanide solution. The cyanide consumption is increased with increasing solubility of minerals and thus the gold dissolution rate decreases.

4.9.2 Effect of Copper Ions

Copper minerals can dissolve to form a variety of copper cyanide complexes such as CuCN, $Cu(CN)_2^-$, $Cu(CN)_3^{2-}$ and $Cu(CN)_4^{3-}$ at appropriate pH values (de Andrade Lima and Hodouin, 2005). The distribution of copper ions and compounds depends on the ratio of cyanide to copper and pH. The formation of $Cu(CN)_2^-$ is preferred at low cyanide concentration and at pH below 6, while high cyanide concentration and high pH are related to $Cu(CN)_3^{2-}$. Hence, copper dissolution is undesirable since it consumes cyanide and oxygen (Marsden and House, 1992). An adequate free cyanide concentration in the solution can prevent the effect of copper. The ratio of cyanide to copper, approximately 3, is presented to be sufficient to remain high gold leaching rate (Marsden and House, 1992; Dai and Jeffrey, 2006). When the cyanide to copper ratio at 2.5 is found, the gold

leaching rate is low (Dai and Jeffery, 2006). Aghamirian and Yen (2005) also presented that copper cyanide at moderate concentrations has a slightly negative effect on gold dissolution.

4.9.3 Effect of Iron Ions

Iron oxides, such as hematite (Fe_2O_3) and magnetite (Fe_3O_4) and iron silicates, are normally insoluble in alkaline cyanide solutions. Iron carbonates, for instance siderite ($FeCO_3$), and other complex carbonate minerals can decompose in low alkalinity solution or pH below 10 but are unreactive at high pH values. Iron sulfides greatly decompose in alkaline cyanide solutions to form iron cyanide complexes and various sulfur species. They are also passivated by the formation of a layer of iron (III) hydroxide on the surface. Consequently, gold particles might be coated and leaching efficiency may be reduced (Marsden and House, 1992). Iron sulfide, especially pyrrhotite ($Fe_{1-x}S$), is a large consumer of cyanide and oxygen since it may form the very stable ferrocyanide ion $[Fe(CN)_6]^{4-}$ (de Andrade Lima and Hodouin, 2005). However, it has been indicated that ferrocyanide ions at high concentration have a positive effect on gold dissolution (Aghamirian and Yen, 2005).

4.9.4 Effect of Lead Ions

In Several studies it has been presented that addition of lead solution for example lead nitrate, $Pb(NO_3)_2$, is able to enhance gold leaching kinetics. Deschênes and Prud'homme (1997) have presented that lead nitrate can act in different ways. They observed that lead nitrate can activate the surface of a passivated gold particle, prevent a passivation film formation on the gold surface and also precipitate the soluble sulfides. Kondos *et al.* (1995) have presented that sulfide mineral, which is distributed in the solution, will be precipitated by excess lead as PbS. Lead ion may also react with gold sulfide film making the passive gold particle to become active again in the absence of sulfide formation. Deschênes *et al*. (2000) have also demonstrated the effect of lead ions in the form of lead nitrate, lead sulfide and lead sulfite, which are reacted with gold and accelerate gold

dissolution. Figure 17 illustrates the effect of adding lead nitrate on gold ore with pyrite, pyrrhotite and chalcopyrite.

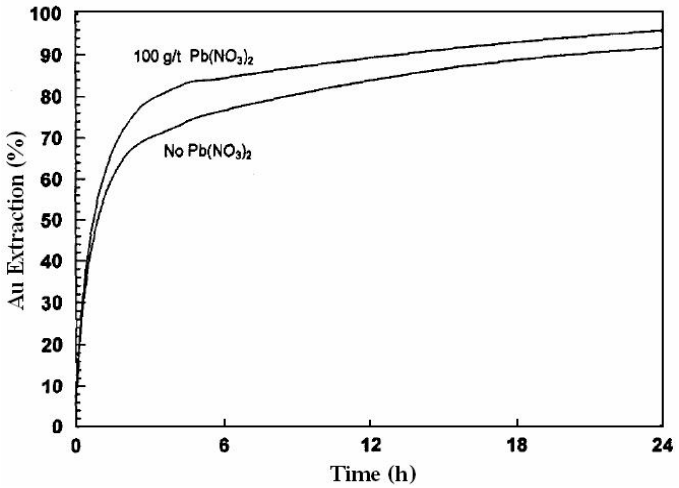

Figure 17 Effect of lead nitrate addition on the leaching of a gold ore with pyrite, pyrrhotite and chalcopyrite (Deschênes *et al*. 2000).

Recently, Breuer *et al.* (2008) have also found that sulfide ion concentration is decreased fast with the addition of lead ions, as shown in Figure 18. They further concluded that lead sulfide might act as a catalyst for sulfide oxidation releasing the lead ions to further react with sulfide ions. Deschênes *et al*. (2003) have shown that the addition of lead nitrate does not affect cyanide consumption.

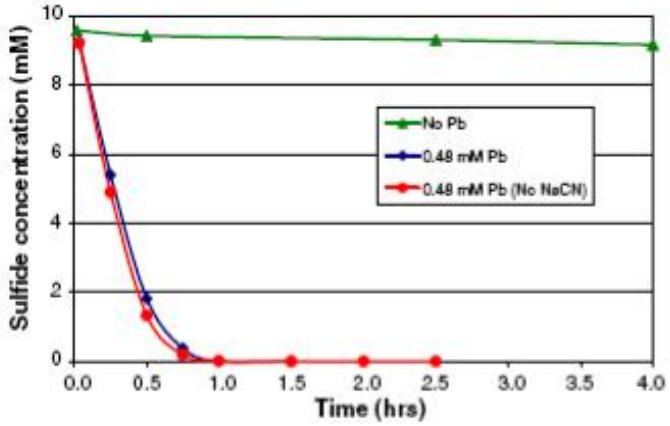

Figure 18 Effect of lead (II) on sulfide oxidation in the absence and presence of cyanide (20.4 mM NaCN, 10 mM S^{2-}, oxygen sparged) (Breuer *et al*., 2008).

However, Kondos *et al*. (1995) also presented that higher concentrations of lead nitrate can reduce gold extraction as shown in the Figure 19. They further discussed that the addition of lead nitrate together with oxygen provides the most effective gold extraction.

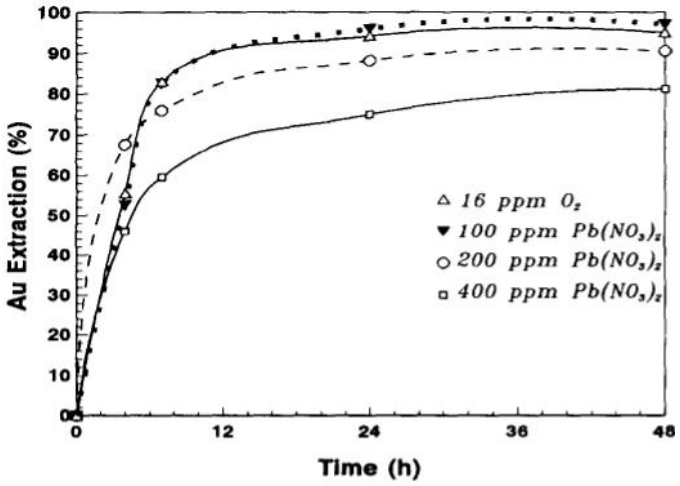

Figure 19 Effect of oxygen and lead nitrate on gold leaching. Condition: [CN^-] = 730 ppm, pH = 11.5, 80% - 74 µm (Kondos *et al*., 1995).

4.10 Presence of Activated Carbon in Pulp

The activated carbon is used as adsorbent in CIP and CIL processes as described in Chapter 5. It may enhance gold leaching from ores by continually removing the leached species from the solution, redistributing the solid/liquid equilibrium and favoring further gold dissolution (Rees and van Deventer, 2000). The chemical and physical properties of the activated carbon affect the adsorption kinetics and the equilibrium gold-loading capacity. According to Ibragimova *et al.* (2007), the most important characteristics of carbon to be predetermined are the kinetic parameter of gold sorption on carbons and the mechanical strength. The adsorption ability has been shown to be dependent upon temperature and cyanide concentration. Marsden and House (1992) have presented the effect of these parameters, as shown in Table 4. It has been observed that increasing the temperature and cyanide concentration reduces the capacity of gold adsorption on carbon.

Table 4 Effect of temperature and sodium cyanide concentration on gold loading (Marsden and House, 1992).

Conditions: Au in solution (pH)	**25 ppm (10.4-10.8)**		
Temperature (ºC)	**Free cyanide (ppm)**	**Rate constant (*k*) (h^{-1})**	**Capacity (ppm)**
20	0	3400	73 000
25	130	3390	62 000
24	260	2620	57 000
23	1300	2950	59 000
44	0	4190	48 000
43	130	4070	47 000
42	260	3150	42 000
43	1300	3010	33 000
62	0	4900	35 000
62	130	4920	29 000
62	260	3900	29 000
62	1300	4060	26 000
81.5	260	5330	20 000

Rees and van Deventer (2000) have also presented the effect of initial cyanide concentration on gold extraction in the presence of activated carbon. This effect is given in Table 5.

Table 5 The effect of 12 g of activated carbon on gold extraction after 22 h of leaching (Rees and van Deventer, 2000).

Initial free CN^- (ppm)	**Extraction without carbon (%)**	**Extraction with carbon (%)**
310	75.0	84.8
135	72.9	78.4
115	68.2	74.3
125	62.6	73.0

It can be seen that the level of cyanide concentration has a slight effect on extraction in both the presence and absence of activated carbon. The gold extraction is enhanced by adding the activated carbon.

Rees and van Deventer (2000) further performed gold extraction for different types of ore, as shown in Table 6. They observed that the presence of activated carbon resulted in an important improvement in the extraction for all ore types.

Table 6 The effect of 4 g of activated carbon on gold extraction at an initial free cyanide concentration of 200 ppm after 24 h (Rees and van Deventer, 2000).

Ore	**Extraction without carbon (%)**	**Extraction With carbon (%)**	**Final $[CN^-]$ (ppm)**
Oxide ore	66.9 ± 2.5	80.4 ± 4	40
Pyrite concentrate	13.2 ± 0.2	16.0 ± 0.2	0
Copper concentrate	1.5 ± 0.02	3.2 ± 0.16	0

The selectivity of activated carbon for gold over other metal cyanide species increases when cyanide concentration is increased (Marsden and House, 1992). Rees and van Deventer (2000) presented that the optimum level of initial free cyanide concentration in the presence of activated carbon is relying on ore type. They found that the improvement of gold extraction in the presence of activated carbon is not strongly dependent on cyanide concentration for the sulfide and copper ores.

5 GOLD CYANIDATION PROCESSES

The adsorption of gold from aqueous solutions onto activated carbon has apparently been known since 1847 (Fleming, 1992). The continuous processes of gold adsorption, namely the carbon-in-pulp (CIP) and the carbon-in-leach (CIL) processes, have been widely used since 1970s (de Andrade Lima, 2007). Marsden and House (1992) have presented in Figure 20 that CIP and CIL processes have been the dominant gold recovery methods in use worldwide, accounting for approximately 44% of world production. Other methods are about 30% for solid-liquid separation and zinc precipitation (CCL & Zn) and 19% for flotation and gravity concentration (MISC). These adsorption processes are significantly used since they avoid the need for solid-liquid separation stages, for example, thickening and filtration, thus can reduce the operating costs (Marsden and House, 1992).

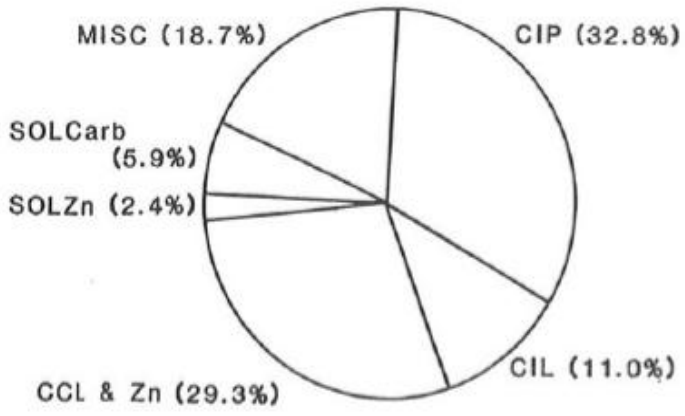

Figure 20 World gold production by recovery method (Marsden and House, 1992).

5.1 Carbon-in-pulp (CIP) Process

Metal recovery or concentration by adsorption onto activated carbon by the carbon-in-pulp (CIP) has become a successful gold extraction technique after milled ore is leached by cyanide solution in aerated alkaline slurries. It comprises

of two main processes which are firstly the leaching step followed by the carbon adsorption as schematically shown in Figure 21.

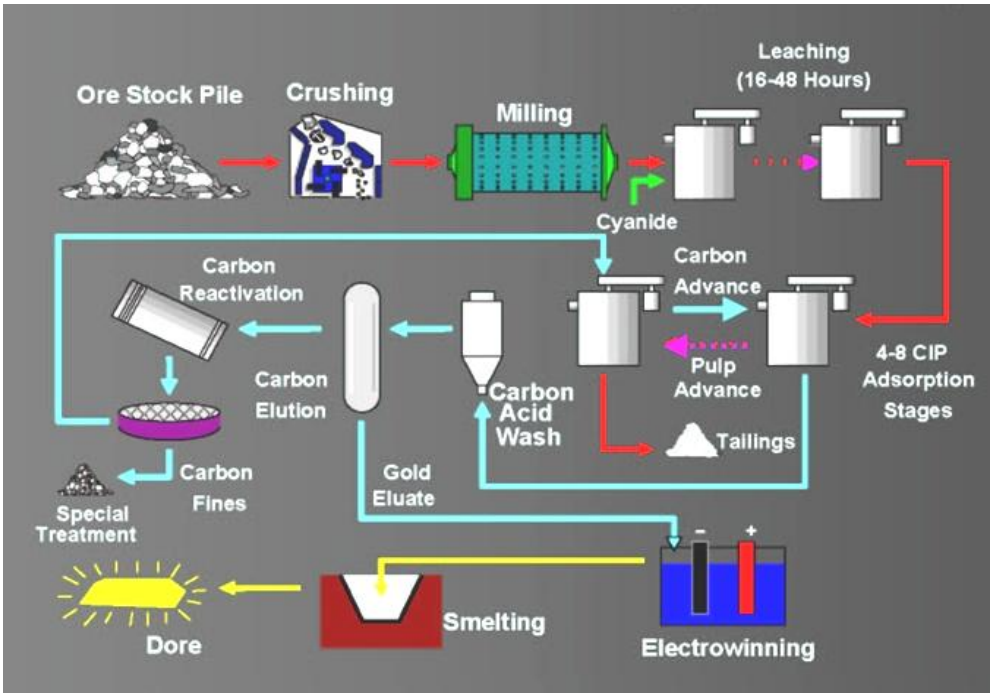

Figure 21 Flow sheet of a modern CIP plant (Fleming, 2004).

5.1.1 CIP Leaching Section

The gold dissolution is largely controlled by the factors such as cyanide and oxygen concentrations, pH and temperature. The high concentrations of oxygen and cyanide improve the gold leaching and thus reduce the residence time and increase throughput (Ellis and Senanayake, 2004).

5.1.1.1 Process Description of CIP leaching section

The ore is first reduced in size (typically 80% passing 75 μm) in crushing and/or ball milling circuit. After comminution the pulp is normally dilute and thickening might be performed to increase the pulp density to about 50% solid by mass. Leaching reagents in the form of cyanide and an oxidant such as air or oxygen are added after thickening (Stange, 1999). The creation of a large number of small oxygen bubbles and dispersing them in the slurry long and deep enough provides adequate oxygen concentration for gold dissolution (Ellis and Senanayake, 2004).

In a typical carbon-in-pulp (CIP) process, the milled ore is leached in a series of agitated vessels, typically about six vessels, each having a retention time of about four hours. The agitated vessels comprise of a conventional mechanical agitator including blades and shaft. The vessels preferably have a cover for the solution to minimize the transfer of oxygen from the slurry to air. The cover can be either a stationary cover or a floating cover, such as a disc-shaped cover which has a generally flat top surface, and generally concave bottom surface which is actually in contact with the slurry. In the agitated leaching reactor the gold is dissolved from the pulp. Pure oxygen or natural air, which can be bubbled into the vessels, is injected at the lower part of the leach tank (Brison *et al.*, 1989). Recently, de Andrade Lima and Hodouin (2006) have investigated the configuration for a gold leaching circuit based on gold price and cyanide cost with five equal-sized reactors. They concluded that for high gold content, 0.5-1.2 mg/kg, and low cyanide concentration, 250-500 mg/dm^3, the conventional in-series configuration is the most recommended. However, for high cyanide concentration, 750-1000 mg/dm^3, and low gold content less than 0.5 mg/dm^3, the in-parallel configuration is economically the most recommended.

5.1.2 CIP Adsorption Section

Activated carbon or activated charcoal is the most widely used as adsorbent due to its efficient properties, for example, large specific surface area of approximately 1000 m^2/g and strong adsorptive capacity (Marsden and House, 1992; Rees *et al.*, 2000). Various types of activated carbon can be used. However, it is often preferred to use activated granular coconut shell carbon because it is harder than most other available types. It is more resistant to breakage and abrasion and has large loading capacity (Kunter and Turney, 1980; Coetzee and Grey, 1999; Yalcin and Arol, 2002). It is widely accepted that gold adsorption onto activated carbon is a complex phenomenon. Many studies have proposed a number of significant mechanisms which can be divided into four categories (Marsden and House, 1992; Vegter, 1992):

(a) Adsorption as Au(I) cyanide ion

(b) Adsorption as molecular AuCN

(c) Reduction and adsorption as metallic gold

(d) Adsorption in association with a metal cation such as Ca^{2+}

The mechanism of gold recovery from cyanide liquors is presented in Equation (34). The dissolved gold cyanide is adsorbed as the cation gold cyanide ion pair (McDougall, 1985; Marsden and House, 1992; Vegter, 1992):

$$M^{n+} + nAu(CN)_2^- \rightleftharpoons M^{n+}[Au(CN)_2^-]_n \quad (34)$$

where the ion pair, $M^{n+}[Au(CN)_2^-]_n$, is the adsorbed gold species. M can be H, Na, K and Ca. The rate steps are the mass transfer of gold cyanide and cations across the solution film surrounding the carbon particles to the outer surface of the carbon particles, transfer in the solution filling the pores, the adsorption reaction and possibly transfer of the adsorbed cation gold cyanide ion pair along the pore walls by surface diffusion (Vegter, 1992). It has been claimed that film transfer controls the adsorption rate of aurocyanide onto the activated carbon in the initial stages of gold recovery (Coetzee and Gray, 1999).

The equilibrium of the adsorption reaction is influenced by many factors, for example, temperature, gold cyanide concentration, presence of organic solvent, type of cations in the solution and the ionic strength of the solution (Vegter, 1992). In the initial rate of gold adsorption, gold is adsorbed on the surface of macropores and possibly mesopores in activated carbon at a high rate. After that the adsorption rate decreases as equilibrium is approached, as shown in Figure 22.

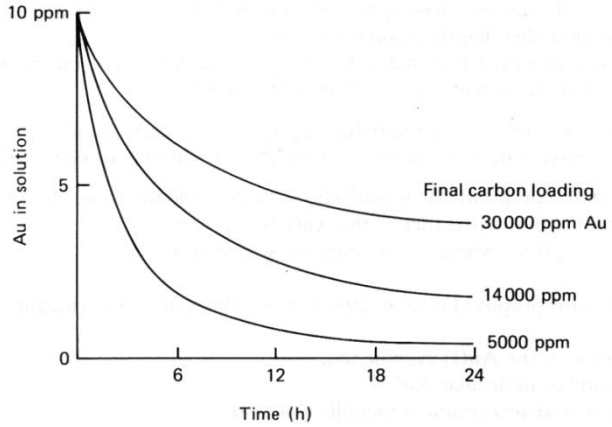

Figure 22 An example of kinetics of gold loading onto activated carbon (Marsden and House, 1992).

Marsden and House (1992) have presented a first-order rate equation for gold adsorption onto carbon as follows:

$$\log C_{Au,L}(t) = k_{ads}\, t + \log C_{Au,L}^{ini} \tag{35}$$

where $C_{Au,L}(t)$ gold concentration in solution at time t, mg/dm^3

$C_{Au,L}^{ini}$ initial gold concentration, mg/dm^3

k_{ads} rate constant for gold adsorption, s^{-1}

Ibragimova *et al.* (2007) have also presented a first-order reaction where the rate constant k_{ads} of $[Au(CN)_2]^-$ ion adsorption on activated carbon is presented as shown in the following equation:

$$dC_{Au,C} / dt = k_{ads}\, C_{Au,L} \tag{36}$$

where $C_{Au,C}$ and $C_{Au,L}$ are the gold concentrations in the carbon and solution phases, respectively and the adsorption rate constant, k_{ads}, is dependent on a multitude of parameters. Coetzee and Grey (1999) have presented a typical adsorption profile for the recovery of aurocyanide by the activated carbon in a batch reactor as shown in Figure 23, indicating the regions and points of importance. The diminishing aurocyanide decay period replaces the constant rate adsorption when the rate of intraparticle diffusion becomes the rate controlling factor (Coetzee and Grey, 1999).

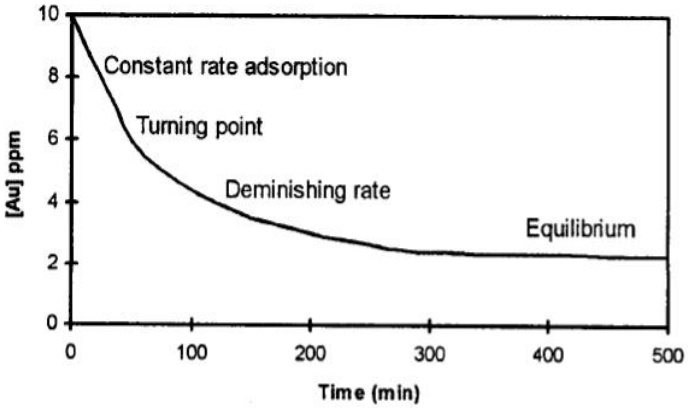

Figure 23 A typical adsorption profile of aurocyanide onto activated carbon (Coetzee and Grey, 1999).

The equilibrium isotherm is further illustrated in Figure 24. It is an empirical equation relating the concentration of the chemical species in the liquid phase to their concentration on the surface of the activated carbon.

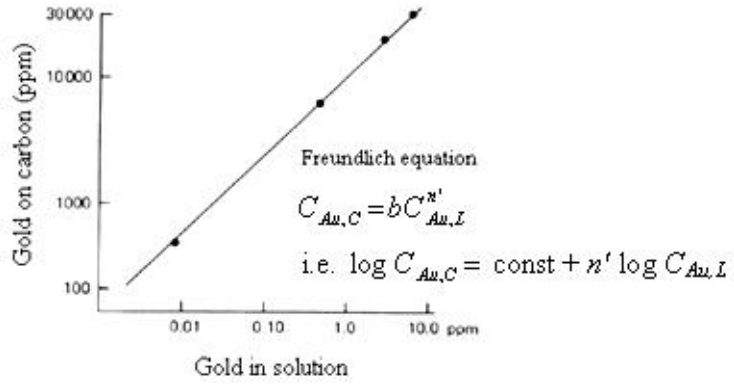

Figure 24 Equilibrium adsorption isotherm for loading of gold on carbon (Marsden and House, 1992).

An empirically developed equilibrium gold loading capacity (K value) has been suggested to be used for the evaluation of carbons used in gold adsorption systems. It is obtained by contacting various weights of carbon with a standard borate buffer-gold solution for a fixed time. The K value is interpolated as the carbon loading in equilibrium with a residual gold solution concentration of 1 mg/dm^3 (Marsden and House, 1992). Figure 24 shows the Freundlich isotherm which has been used to depict gold adsorption on activated carbon. $C_{Au,C}$ represents the gold

concentration in carbons, $C_{Au,L}$ is the gold concentration in solution, *b* is the Freundlich adsorption constant and *n'* is the Freundlich exponent. In the case of *n'* = 1, the Freundlich isotherm reduces to linear isotherm which is accurate for low concentration systems, as is usually true for this case. The Langmuir isotherm is also used to describe gold adsorption (de Andrade Lima, 2007).

5.1.2.1 Process Description of CIP adsorption section

After leaching, the pulp is then introduced to the CIP adsorption process. The CIP consists of three essential stages (Marsden and House, 1992; de Andrade Lima, 2007):

(a) Adsorption: the dissolved gold in the pulp is loaded onto activated carbon

(b) Elution: gold is removed from carbon into an alkaline cyanide solution

(c) Electrowinning: gold is removed by an electrical process from the alkaline cyanide solution and deposited on electrodes.

The CIP adsorption process occurs continuously in a cascade of large agitated tanks, typically approximately six vessels each having a retention time of about one hour. Conventional components of the vessel include the mechanical agitator including blades and shaft, the slurry inlet and outlet covered by a screen and the carbon inlet and outlet. Non-conventional components of the tank also include a sparger located adjacent the tank bottom for sparging oxygen into the tank in order to enhance adsorption efficiency onto the activated carbon (Brison *et al.*, 1989; Marsden and House, 1992). Another non-conventional vessel comprises of top sealing in the tank in order to maintain an oxygen atmosphere of about one atmosphere pressure, or significantly greater (Brison *et al.*, 1989). The pulp is agitated and flows by gravity from one tank to the next by overflow. The solution first comes into contact with the activated carbon in the first tank. The fresh or reactivated carbon is introduced at the tail end of the process and is countercurrently transferred either continuously or periodically with respect to the pulp. The carbon in each stage becomes loaded to pseudo-equilibrium, depending on the gold concentration in the solution in each stage. In the first stage, the carbon

has the highest gold loading and it is contacted with the highest concentration of the solution and vice versa. The slurry is discharged through the outlet of the tank to a disposal site for the ore tailings. The gold containing carbon is treated by an elution step to desorb the metals which are further recovered in electro-winning process. The eluted carbon is regenerated with acid to remove the contaminants. After that it is recirculated into the adsorption-elution circuit.

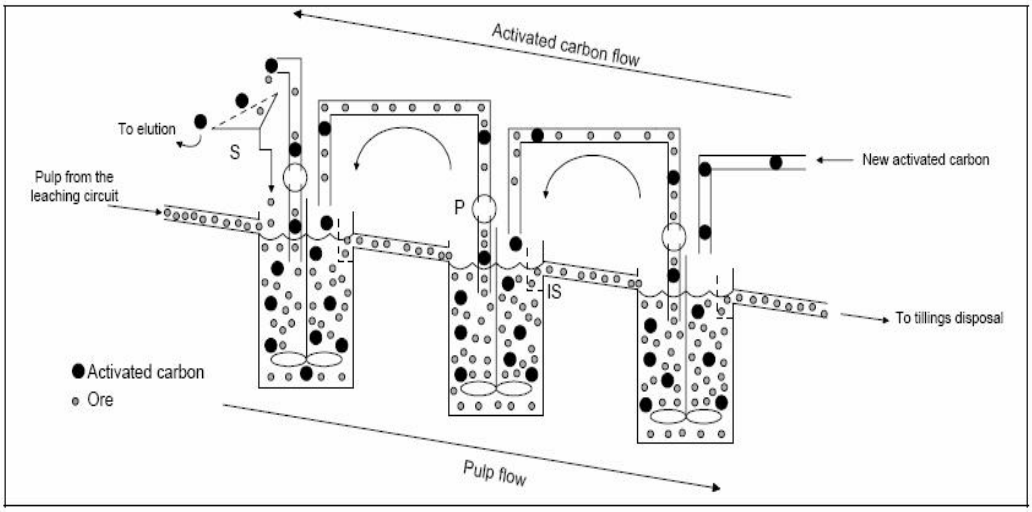

Figure 25 Schematic diagram of a carbon-in-pulp or carbon-in-leach process with three tanks, showing inter-stage screens (IS), the screen at the exit of the first tank (S), and the carbon transfer pumps (P) (de Andrade Lima, 2007).

The process involves the use of inter-stage screens (IS) where carbon is retained in each adsorption stage due to the fact that it is much larger than the ore particles. Figure 25 depicts the inter-stage screens at the reactor exit that confine the carbon in the tanks until the transfer of pulp is activated. The screens have apertures which are slightly smaller than the activated carbon but large enough to allow free flow of the slurry between the stages, typically 0.6-0.8 mm (Stange, 1999). The efficiency of inter-stage screening has received much attention since it is claimed to be one of the biggest challenges in the application of carbon adsorption.

The activated carbon can be used in a variety of size ranges, usually 1.7 × 3.4 mm, 1.2 × 3.4 mm and 1.2 × 2.4 mm. The tanks normally contain of 10-25 grams of

carbon per liter of pulp (0.5 to 1.2% by volume carbon). Loaded carbon values on operating plants range from 300 to 20,000 grams of gold per ton of carbon (Marsden and House, 1992).

5.2 Carbon-in-leach (CIL) Process

Conventional carbon-in-leach (CIL) process is similar to the CIP process except that the leaching and adsorption steps take place in the same tanks simultaneously. Carbon is added in the leach tank so that gold can be adsorbed onto carbon almost as soon as it is dissolved by cyanide solution. The CIL process is mainly used to treat ores containing organic matter and preg-robbing species that are able to adsorb $[Au(CN)_2]^-$ anions from solution by carbonaceous species in ore, clay-type minerals and other mineral species such as graphite (Marsden and House, 1992; Rees and van Deventer, 2000; van Deventer *et al*., 2004; de Andrade Lima, 2007; Ibragimova *et al*., 2007). The process has the advantage of lower capital investment cost than separate leaching and carbon adsorption systems and it also improves gold extraction by the presence of carbon. The CIL process is a good alternative, but there are also some disadvantages. For example, it requires a larger carbon inventory resulting in a larger in process tie-up of gold. Carbon and gold losses due to carbon attrition are higher and carbon loading will be lower than in CIP process, meaning that more carbon has to be stripped (Marsden and House, 1992).

In a typical CIL technique, the ground and thickened ore slurry typically passes to a series of about six agitated vessels, each having a retention time approximately four hours (Brison *et al*., 1989). Figure 26 schematically illustrates the CIL process. The activated carbon is mixed with the ore pulp in an agitated leach tank. A counter-current flow is maintained between the gold ore slurry, containing gold cyanide and oxygen in solution, and the activated carbon. The leached slurry flows down the cascade while carbon is transferred periodically upstream. In the first tank of the series, leaching of the fresh pulp is a primary activity. In the latter tanks, adsorption onto the activated carbon is dominant as the concentration of

gold in the solution increases and the fresh carbon is loaded into the system. The pulp then passes through the carbon inter-stage screens the same manner as in the CIP process shown in Figure 25. The aperture of the inter-stage screens allows the leached pulp to pass through by gravity. The loaded carbon then passes to a loaded carbon screen where the slurry is screened. The carbon is further stripped and thermally regenerated to restore the active surface and to increase adsorption activity before reuse. The gold solution moves to electrowinning process where gold and other metals are precipitated on steel wool cathodes (Brison *et al*., 1989; U.S. Protection Agency, 1993; van Deventer *et al*., 2004).

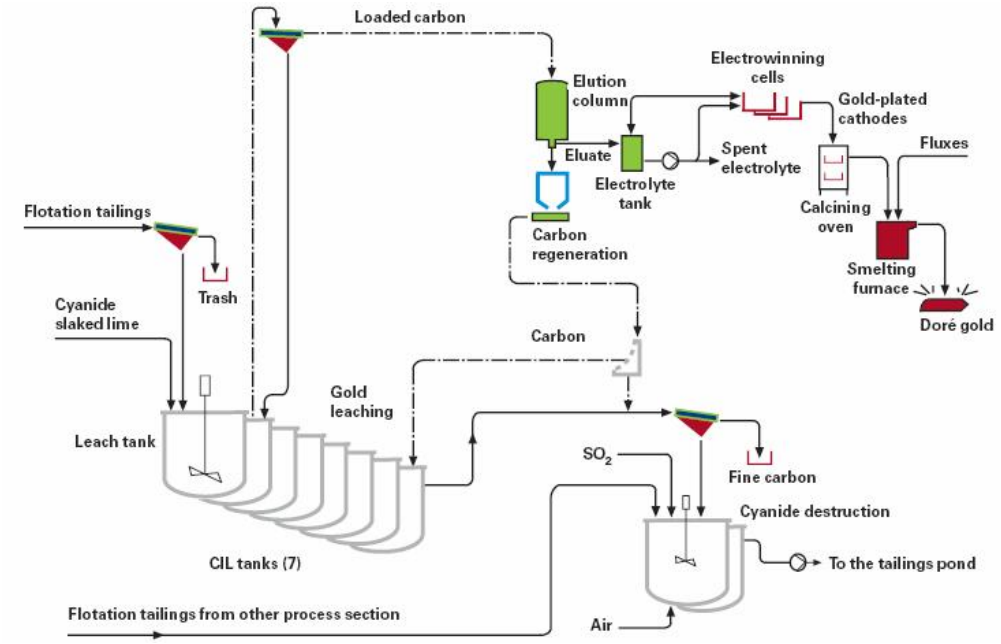

Figure 26 The carbon-in-leach process (Outokumpu, 2004).

According to Brison *et al.* (1989), typical conditions of the ore slurry would be 50% solids (-100 mesh), solid specific gravity of 2.7 and slurry specific gravity of 1.46. They also experimented with oxygen atmosphere, pH 9-11, 0.3 grams of NaCN per liter. The results show the gold leaching in the range of 91-92% in six hours and low cyanide consumption.

5.3 Cyanidation at High Pressure and/or Elevated Temperature

The direct oxidative pressure cyanidation has been recently presented as a new technology where high pressure is a main operating condition. This improved technique is applied in autoclaves where oxidation and dissolution of gold can take place simultaneously. Several metallurgical plants under projects, for example, Goldstrike, McLaughin, Campbell Red Lake, have successfully used pressure leaching as pretreatment of refractory gold ores (Fleming, 1992). This high pressure leaching can treat pyrite refractory gold concentrations as well. The decomposition products of the oxidation of refractory gold ore are dissolved species and can be precipitated under certain condition. The partial decomposition reactions of refractory gold ore are presented as follows (Fleming, 1992; Parga *et al*., 2007):

$$2FeS_2 + 7O_2 + 2H_2O \rightarrow 2Fe^{2+} + 4SO_4^{2-} + 4H^+ \quad (37)$$

$$FeS_2 + 1/2O_2 + 2H^+ \rightarrow 2Fe^{3+} + H_2O \quad (38)$$

$$Fe_7S_8 + 32H_2O + 62Fe^{3+} \rightarrow 69Fe^{2+} + 64H^+ + 8SO_4^{2-} \quad (39)$$

$$2FeAsS + 7O_2 + 2H^+ + SO_4^{2-} + 2H_2O \rightarrow 2Fe^{3+} + SO_4^{2-} + 2H_3AsO_4 \quad (40)$$

The reactions taking place at high pressure also provide the formation of elemental sulfur layer and thus allowing cyanide and dissolved oxygen to enter the locked gold (Parga *et al*., 2007).

Recently Lorenzen and Kleingeld (2000) have presented a novel jet reactor technology, with specific regard to gas-liquid-solid cyanidation system using gas-liquid jet reactor and solid-liquid jet reactor. They also presented gas-liquid jet reactor designs which were determined to be the most efficient configuration as shown in Figure 27. The design is for bringing gas into contact with liquid, using high levels of turbulence and impingement zone.

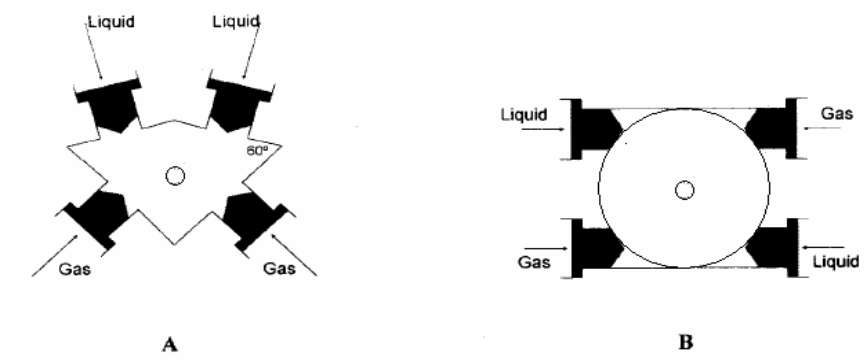

Figure 27 Simplified diagrams of the gas-liquid reactor designs: (A) Kite-shaped reactor and (B) σ-shaped reactor (Lorenzen and Kleingeld, 2000).

The result shows that a gold recovery of 99% was achieved after only 2½ hours of contact time when using solid-liquid reactor under condition of 1 kg KCN/t, pH 10 and high pressure at 20-30 MPa. They concluded that these new jet reactors connected in series can be used in cyanidation process to increase gold recovery (Lorenzen and Kleingeld, 2000).

5.3.1 Operating Conditions

It has been found that the oxidative pressure cyanidation can be carried out at temperature below about 120 ˚C and at pressure about 1000 kPa (Corrans *et al*., 1993; Hourn *et al*., 1999). Sundkvist (2002) has presented that the high yield of gold recovery, 95% approximately, was obtained in several trials at a temperature of 60-80 ˚C. The best condition for gold production has been found at a temperature of 75 ˚C, at pH 11-11.5. Parga *et al*. (2007) also experimented at operating conditions of 60-200˚C, 1% NaCN, PbO 100 g/t, 0.6 MPa oxygen pressure and at pH 11.2. The results show that increasing the temperature above 80˚C decreases the gold extraction since the oxidation of cyanide ions is too rapid. This results in the formation of CO_2 gas and ammonium ions. Consequently, at these conditions with the residence time of 60 min the gold recovery exceeds 96%. Figure 28 illustrates the percentage of gold extraction at operating conditions compared to ambient conditions.

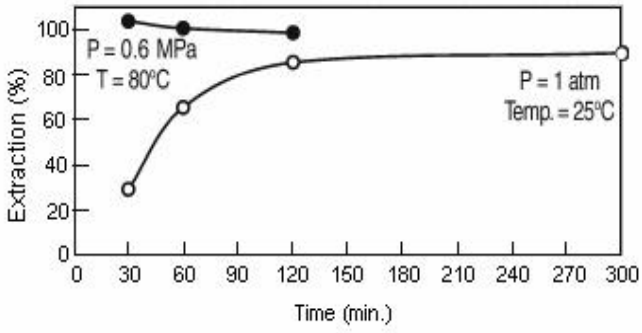

Figure 28 A comparison of gold extraction at ambient conditions and high pressure. Condition: % solid = 20; pH = 11; speed = 300 min^{-1} (Parga *et al*., 2007).

5.4 Intensive Cyanidation

Intensive cyanidation is a proven technology operating at high gold and reagent concentrations and/or high temperature and pressure to increase gold dissolution rate. The intensive cyanidation is applied for gravity concentrates containing coarse gold. Oxygen may be introduced as air, pure oxygen or mixture of the two to gain elevated oxygen partial pressure (Marsden and House, 1992). Table 7 presents the different leaching conditions between the intensive cyanidation and conventional one.

Table 7 Comparison between leaching conditions in intensive and conventional cyanidation (Longley *et al*, 2003).

Conditions	Intensive cyanidation	Conventional cyanidation	Factor
Au, g/t	20,000	2	10,000
CN, ppm	20,000	500	40
O_2, ppm	15	8	2
Au dissolution rate, g/h/t	1000	0.1	10,000

The conventional methods such as high-speed agitator in a tank and vat leaching have shown problems due either to excessive wear and high energy requirement for the agitated systems and loss of fine gold in the vat type systems resulting in poor recoveries. Gold recovery on the production tables is relatively low, often between 30 % and 60 % (Longley *et al*., 2003). Many researchers, therefore, have

attempted to develop new machines that can very efficiently and economically concentrate gold by gravity. Both the ConSep ACACIA Reactor and Gekko System's InLine Leach Reactor are widely used in intensive cyanidation, with gold recoveries more than 95 % (Mineral Engineering International, 2005). These new devices are able to bring down the operating costs as well.

5.4.1 ACACIA Reactor

The ACACIA Reactor is widely known as The ConSep ACACIA Reactor, shown in Figure 29, where ConSep is the supplier. This reactor is a high efficiency leaching device using a high intensity cyanidation method to achieve very high recovery. The process consists of an upflow fluidized reactor, which has been developed to produce ideal solid-liquid interaction in order to maximize gold leaching reaction kinetics without mechanical agitation. The product from the process is in the form of cathode gold which is ready for traditional smelting step (Campbell and Watson, 2003).

Figure 29 The ConSep ACACIA Reactor (Consep Pty Ltd).

5.4.1.1 Process Description

Figure 30 presents the basic flow sheet of the ACACIA Reactor.

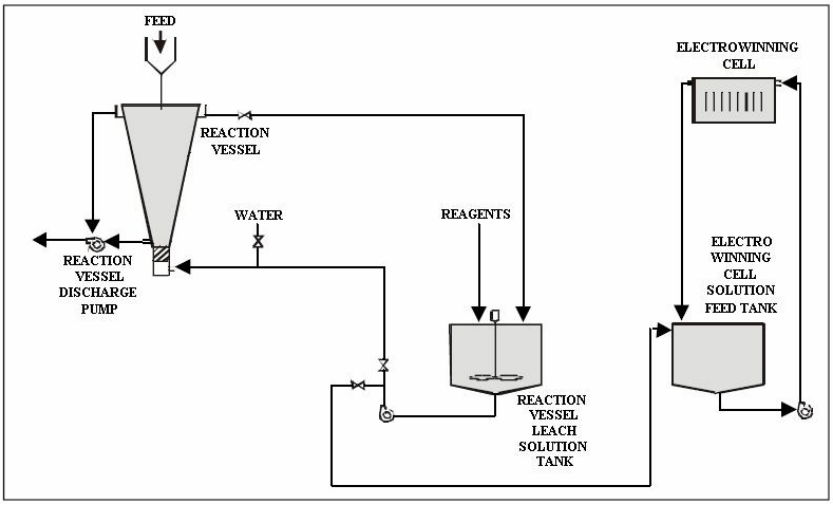

Figure 30 Basic flow sheet of the ACACIA Reactor (Watson and Steward, 2002).

The ACACIA is operated in batchwise. The gold concentrate is pre-washed to remove suspended solids that maybe entrained in the gravity concentrate and may interfere with the subsequent gold electrowinning. The concentrate solids are then fluidized for 30 minutes, approximately. The fine solids are introduced into the upflow of the leach solution which is pumped at a rate sufficient to fluidize the concentrate. The leach solution is mixed in the Reaction Vessel Feed Tank. The concentrated cyanide (NaCN), caustic soda and portable water are added into the tank. Typically high leach recoveries can be achieved in less than 8 hours. The leach cycle must be completed within 16 hours. The pregnant solution is then transferred to the main eluent tanks for eletrowinning (Watson and Steward, 2002).

According to the experiment of Watson and Steward (2002) at temperature between 50 to 65 ºC with H_2O_2 and non oxygen based oxidant, the results show that the gold in the gravity concentrate is recovered over 98% within 8 hour leach time at any condition as shown in Figure 31. The forth case provides the highest gold recovery, 99.8% under condition of 80 liters of solution, 1600 grams of cyanide, 280 grams of NaOH and concentrate grade of 1.5% Au.

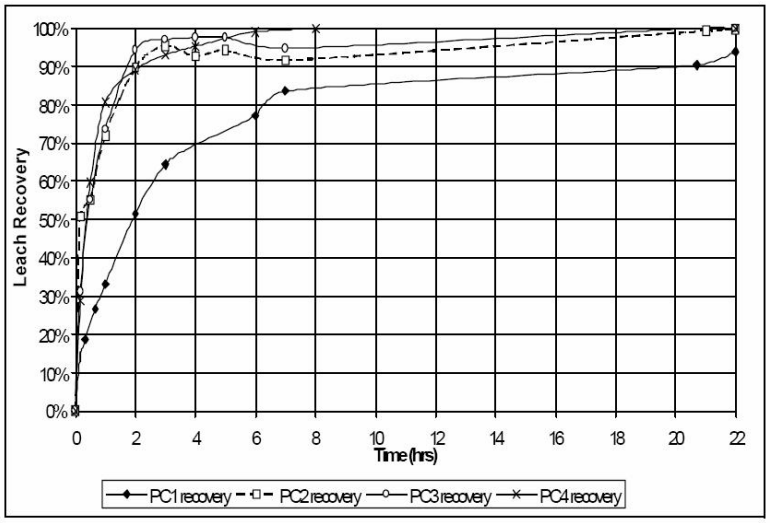

Figure 31 Recoveries during commission at different conditions in ACACIA Reactor (Watson and Steward, 2002).

5.4.2 InLine Leach Reactor

The InLine Leach Reactor (ILR) is a commercial, either continuously or batch wise operate intensive cyanidation reactor. The batch models of the InLine Leach Reactor have been developed to treat higher-grade concentrates between 1000 and 20,000 g Au/t, while the continuous InLine Leach Reactors have been developed to treat lower-grade concentrates above 50 g Au/t. This allows flexible application of the intensive cyanide leaching technology for the treatment of different primary concentrates. Oxygen gas or peroxide can be used as the oxygen source. Typically, the level of dissolved oxygen is above 20 ppm, pH at 13.5 and the cyanide level is 2% or 20,000 ppm (Katsikaros N., Gekkos System Pty Ltd, private conversation, 2008). The leach times range from 6 hours up to 24 hours (Gray, 2000). Figure 32 illustrates the area of application for each type of ILR in relation to concentrate mass and Au grade.

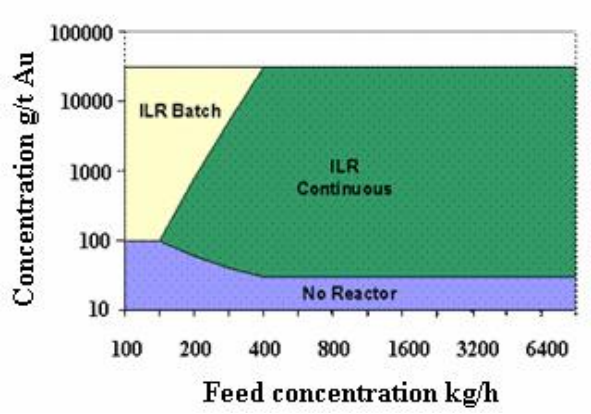

Figure 32 Areas of application of the continuous and batch ILR (Gekko Systems Pty Ltd).

The commercial name for the reactor is Gekko's System InLine Leach Reactor where Gekko is a manufacturer. The ILR works on the principle of laboratory bottle roll to keep the solids in contact with the reagents. It consists of a horizontal drum rotating at approximately 1 min^{-1}. This allows the reactor to agitate and leach coarse material, typically up to 6 mm, at high percent solids. The solids are not suspended in the reactor as in typical slurry but they are well mixed so that all solids and solution are contacted and the reagents are intimately mixed (Katsikaros N., Gekkos System Pty Ltd, private conversation, 2008). Figure 33 presents a typical of the InLine Leach Reactor.

Figure 33 InLine Leach Reactor, model ILR 2000 (Gray, 2000).

5.4.2.1 Process Description of the Batch InLine Leach Reactor

The concentrates from primary recovery device are fed to the feed cone for de-watering. The solids are stored in the feed cone until the beginning of each leach cycle. The reagents are added and stored in the solution storage tank. During the leaching step the solution containing the reagents is continually recirculated from the solution storage tank to the reactor feed. The solution is then overflown to the sump before being returned to the solution storage tank. Figure 34 shows the flowsheet of the Batch InLine Leach Reactor.

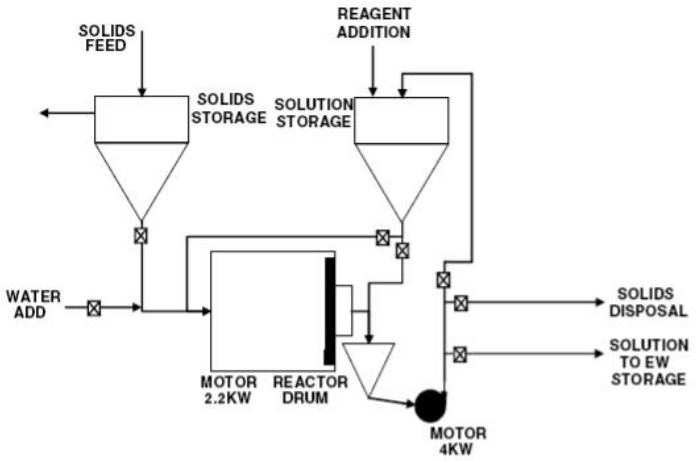

Figure 34 Batch InLine Leach Reactor flowsheet (Longley *et al*., 2003).

The reactor drum is horizontally rotated only fast enough to ensure that fresh solution is mixed through the solid. The action of the rotating drum draws air into the slurry in order to ensure that no portion of the solids can become oxygen depleted resulting in no occurrence of gold re-precipitation onto steel particles. During drum loading all solids are retained within the leaching system. At the completion of leaching the drum is stopped and the solution in the drum is drained into the sump and further pumped to the solution storage tank. Some fines particles are carried through the drum and recirculated with the solution. The solution is then drained from the bottom of the tanks conical base. Wash water is added to the drum to wash entrained pregnant solution from the solids and drained out then clarified. The leached washed solids are emptied from the drum by reversely rotating the drum. The solids then move to the sump while water is continuously added to pump back to the mill circuit. The pregnant solution can either be

transferred into the dedicated electrowinning tank and cell recovery or directly added into the elution circuit for recovery in the main plant electrowinning cells (Longley *et al.*, 2003). Figure 35 presents the leach and electrowinning performance of the Batch InLine Leach Reactor from the gold mine in Indonesia, with 10 ppm of oxygen, 24 hours operating cycle.

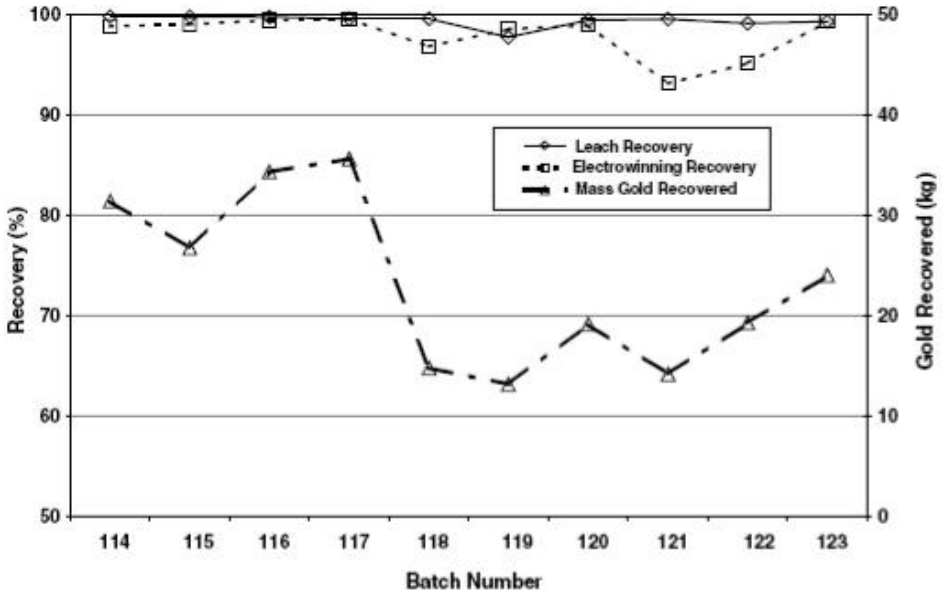

Figure 35 Leach and electrowinning results for Indonesian ILR2000BA (Longley *et al*., 2003).

The results show very high recoveries with an average of 99.5% gold dissolution in the gravity concentrate. Gold electrowinning recoveries averaged 98% on the leach solutions, from gold feed grades of approximately 10,000 g/t. Residue grades of 50 g/t are regularly obtained (Longley *et al*., 2003).

5.4.2.2 Process Description of the Continuous InLine Leach Reactor

The ILR operates continuously in conjunction with an existing or dedicated electrowinning cells with the barren solution recycled back to the ILR to minimize the use of reagent. The continuous intensive cyanide process including the ILR and the dedicated electrowinning cell is shown in Figure 36.

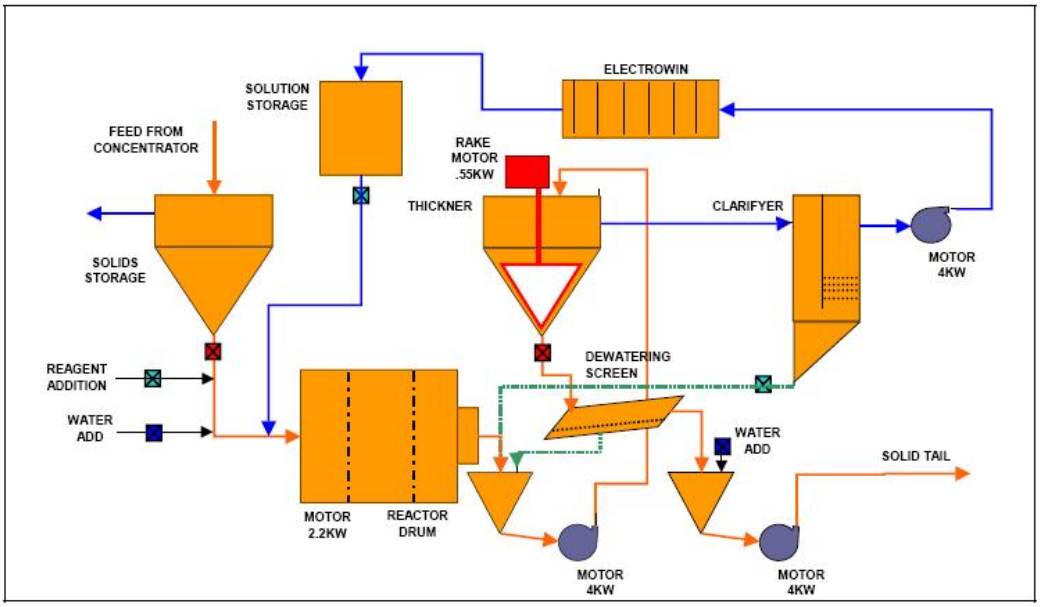

Figure 36 Continuous intensive cyanide process (Gray *et al.*, 2003).

The feed slurry is introduced to the feed cone where it is continuously dewatered. The cone holds the solids and water is overflowed to the ILR tails sump. The thickened feed is then introduced to the reactor drum. Fresh reagents and return barren solution from the eletrowinning circuit are added in the feed. The drum rotates only fast enough to ensure that fresh solution is mixed through the solids. Solution and solids then move to the pregnant solution sump which is divided into three interconnected sections. The first section allows the solids and solution to be pumped to the tails settling cone. The solids settle at the cone bottom and are thickened then moved to the inclined dewatering screen. The solids are dewatered about 83% by weight and dropped from the end of screen into the tailings discharge sump. Any underflow solids from this screen are returned to the pregnant solution sump. The overflow from the tailings settling cone goes to the second section of pregnant section sump. The third section incorporates a set of lamella plates to complete the clarification of liquor. The overflow from the lamella plates is then pumped to the solid settling vessel to ensure that the minimal solids reach the electrowinning cell. Flocculent may be used to improve the clarification performance. The barren solution overflows from the tail of electrowinning cell and is returned back to the feed of reactor drum. The system provides excess

solution, which is released as overflow from a small tank located at the reactor feed (Gekko System Pty Ltd.).

Longley (2004) has investigated the gold leach performance using technology combined gravity/flotation concentrate prior to ILR intensive cyanide, with 0.5 % cyanide concentration and 40 ppm dissolved oxygen levels. This combining method was found to be efficient since it decreased capital costs and improved safety due to reduced cyanide consumption. The results show that 92.9 % gold recovery was obtained after 8 hours and 95.9 % after 24 hours.

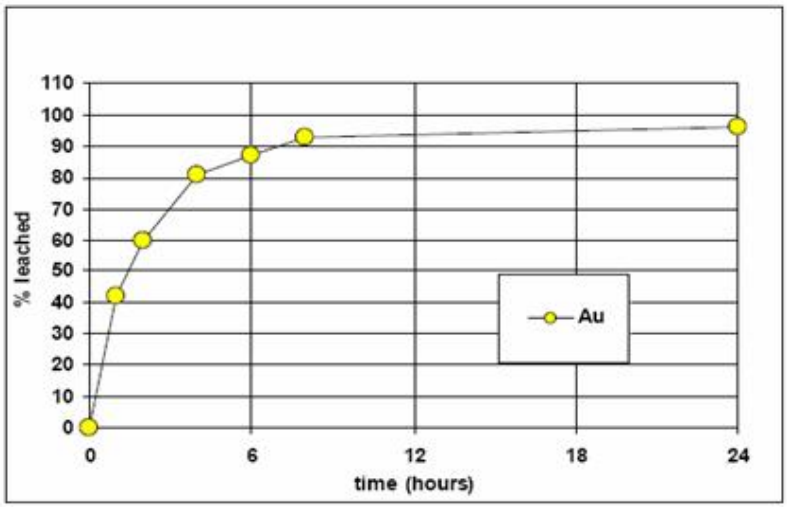

Figure 37 ILR intensive cyanide leach recovery curve (Longley, 2004).

6 GOLD CYANIDATION MODEL

In this work, a numerical model for gold leaching is developed to improve the reliability of the model predictions. The model takes into account the effects of surface reaction, internal diffusion and decreasing of active surface area during the leaching. A numerical shrinking-core model (SCM) is considered since it is flexible to use with multiple reactions and its kinetic model can be developed with different reaction orders. Furthermore external mass transfer limitations can be easily involved in numerical models. For shrinking-core model, the zone of reaction moves into the solid, leaving behind the completely converted material. Thus, at any time there exists an unreacted core of material which shrinks in size during reaction (Levenspiel, 1999).

6.1 Assumptions and Approximations for Gold Leaching Model

Leaching is a heterogeneous reaction which includes the decreasing of surface area as the reaction proceeds. In order to develop the model of gold cyanidation, the followings simplifying assumptions are taken as below.

1. The system of gold cyanidation is assumed to be well mixed so that the solid-liquid mass transfer resistances can be neglected.
2. The reactions taking place follow Equation (7) where no side reactions are taken into account.
3. The leaching reaction is assumed to take place inside the spherical particle so the shrinking-core model is considered as shown in Figure 38.
4. The cyanide concentration is in excess when compared to oxygen concentration. Therefore, the concentration of cyanide at the reacting surface does not have to be solved.
5. Pseudo steady-state conditions are assumed inside the particle and the particle concentration profiles are independent on time.

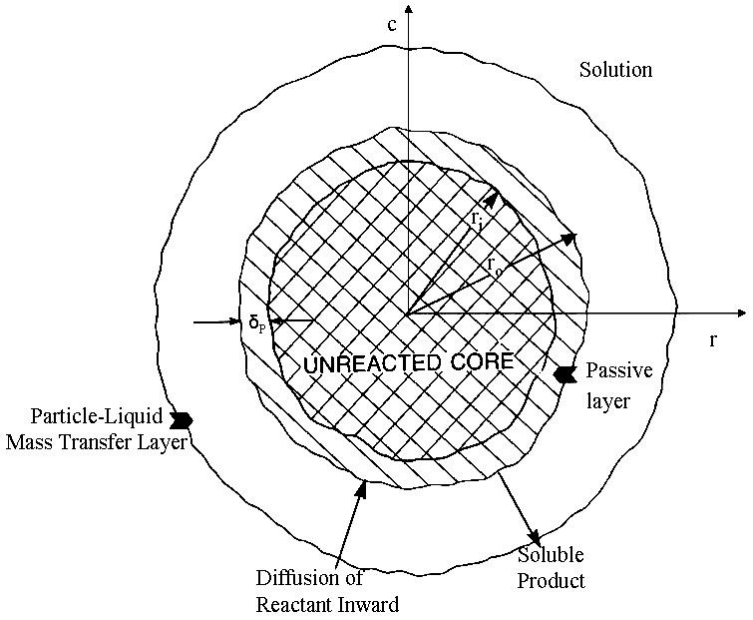

Figure 38 Illustration of the reacting surface and passive layer in the shrinking-core model: δ_P is the thickness of the passive layer.

6.2 Kinetic Model for Gold Leaching

In this current study, two leaching rate equations are used to describe the gold cyanidation kinetics. The leaching is normally presented as the amount of metal extraction over time (the metal extraction curve). The rate equation can be expressed with a term for each reactant as follows:

$$r_s = kC_{CN^-}^{\alpha} C_{O_2}^{\beta} C_{Au,s}^{\gamma} \qquad \text{mol m}^{-2}\,\text{s}^{-1} \qquad (41)$$

where $C_{Au,s}$ surface concentration of gold in particle, mol/m^2

C_{CN^-} cyanide concentration, mol/m^3

C_{O_2} oxygen concentration, mol/m^3

k overall rate constant, unit depends on reaction orders

r_s reaction rate at surface, mol/m^2 s

The reaction of gold is considered as a surface reaction. Gold dissolution begins when the gold in the particles reacts with the reagents at the particle surface. The

dissolved gold diffuses out of the particle due to solution concentration gradient. According to the shrinking-core model as illustrated in Figure 38, a passive layer is formed on the particle surface above the reactive surface. The thickness of the passive layer will continually increase as the reaction proceeds. Oxygen diffuses from solution through this layer to the reactive surface. In the rate equation it may be assumed that the gold concentration at the particle surface is constant at any time since it is characteristic to the concentrate. Consequently, the reaction rate constant, k, and gold concentration, $C_{Au,s}$ can be lumped, as given:

$$r_s = k_1 C_{CN^-}^{\alpha} C_{O_2,s}^{\beta} \qquad \text{mol m}^{-2}\,\text{s}^{-1} \qquad (42)$$

where $C_{O_2,s}$ oxygen concentration at the reacting surface, mol/m^3

k_1 overall reaction rate constant, unit depends on reaction orders

Another kinetic equation is obtained if the reaction rate is assumed to depend also on the gold concentration in the particles. Some amount of gold in the particles remains unreacted thus the non-reacting gold should be removed from the total gold concentration in the model. The gold concentration is presented as the difference of gold concentrations between its concentration and its residual gold concentration after infinite leaching time. The rate equation becomes:

$$r_s = k_2 C_{CN^-}^{\alpha} C_{O_2,s}^{\beta} (C_{Au} - C_{Au}^{\infty})^{\gamma} \qquad \text{mol m}^{-2}\,\text{s}^{-1} \qquad (43)$$

where C_{Au} gold concentration in particles, mol/m$_R^3$

C_{Au}^{∞} gold concentration in particles after infinite leaching time, mol/m$_R^3$

k_2 overall reaction rate constant, unit depends on reaction orders

The gold dissolution rate can be given as:

$$\frac{dC_{Au}}{dt} = -r_s A_i n \qquad \text{mol m}^{-3}\,\text{s}^{-1} \qquad (44)$$

where A_i surface area of one particle during leaching, m^2

n number of particles per volume, $1/m_R^3$

The surface area of sphere particle related to shrinking-core model can be calculated as follow:

$$A_i = \pi d_P^2 \left(\frac{C_{Au}}{C_{Au,ini}} \right)^{2/3} \quad (45)$$

where $C_{Au,ini}$ initial gold concentration in particles, mol/m_R^3

d_P particle diameter, m

6.3 Internal Mass Transfer of Oxygen in Gold Leaching

Mass diffusion rates within the porous residue are difficult to assess. This is because it is impossible to define the shape of the channels through which the transfer takes place. However, the rate of the transfer in a spherical diffusion layer can be approximately obtained.

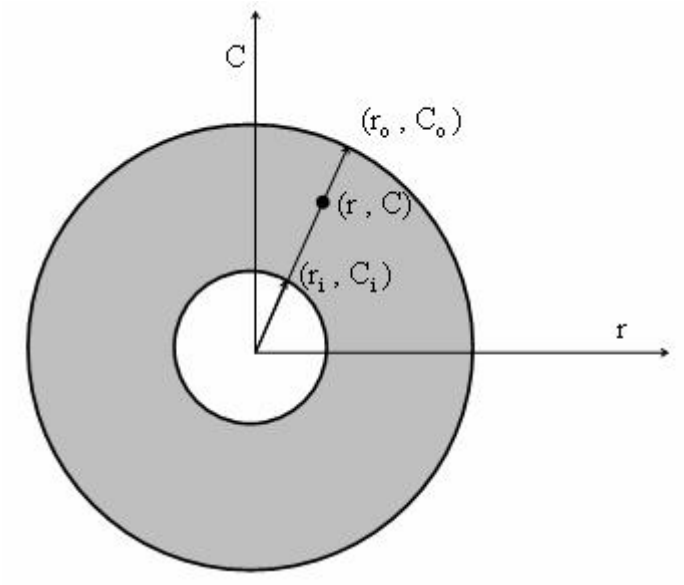

Figure 39 Illustration of a spherical diffusion layer.

The oxygen concentration at the reacting surface can be solved numerically from mass balance under assumption of pseudo-steady state inside the particle. The

following equations present the concentration profile in a spherical diffusion layer as illustrated in Figure 39.

$$Cr(r_o - r_i) = C_i r_i (r_o - r) + C_o r_o (r - r_i) \tag{46}$$

$$C(r) = \frac{C_i r_i (r_o - r) + C_o r_o (r - r_i)}{r(r_o - r_i)} \tag{47}$$

where C concentration in spherical diffusion layer, mol/m_L^3

C_i concentration at inner passive layer, mol/m_L^3

C_o concentration at outer passive layer, mol/m_L^3

r radial coordinate, m

r_i inner radius of passive layer, m

r_o outer radius of passive layer, m

The concentration gradient in the layer is then obtained as follows:

$$\frac{dC}{dr} = \frac{r_i r_o (C_o - C_i)}{r^2 (r_o - r_i)} \tag{48}$$

The equation for mass diffusion rate of oxygen at the inner and outer surfaces can be given in terms of concentration gradient and effective diffusivity (D_e) as shown below:

$$\dot{N}_{O_2} = -D_e A_r \frac{dC}{dr} \quad \text{mol s}^{-1} \tag{49}$$

$$= -D_e A_{r_i} \frac{r_o (C_{o_2} - C_{o_2,s})}{r_i (r_o - r_i)} \quad \text{mol s}^{-1} \tag{50}$$

$$= -D_e A_{r_o} \frac{r_i (C_{o_2} - C_{o_2,s})}{r_o (r_o - r_i)} \quad \text{mol s}^{-1} \tag{51}$$

where A_r reacting surface area of particles, m^2

A_{r_i} inner surface area of passive layer, m^2

A_{r_o} outer surface area of passive layer, m^2

D_e effective diffusivity in particles, m^2/s

$\dot{N}_{O_2}$ diffusion rate of oxygen, mol/s

The radius of the reactive surface r_i is continuously recalculated as the reaction proceeds and gold is leached. According to the shrinking-core model, the reactive surface decreases as the reactive layer penetrates deeper and deeper into the concentrate particle. Therefore, the active area in Equation (44) continually reduces as the reaction proceeds.

The steady state diffusing rate is equal to the rate of reaction of oxygen within the reaction zone. Therefore, the mass balance for oxygen at the reacting surface can be obtained and oxygen concentration at ore surface can be solved for Equations (42) and (43) as presented, respectively:

$$0.25k_1 C_{CN^-}^{\alpha} C_{O_2,s}^{\beta} A_i = D_e A_{r_o} \frac{r_i (C_{O_2} - C_{O_2,s})}{r_o (r_o - r_i)} \tag{52}$$

and

$$0.25k_2 C_{CN^-}^{\alpha} C_{O_2,s}^{\beta} (C_{Au} - C_{Au}^{\infty})^{\gamma} A_i = D_e A_{r_o} \frac{r_i (C_{O_2} - C_{O_2,s})}{r_o (r_o - r_i)} \tag{53}$$

where the value of 0.25 is the stoichiometric constant of oxygen referring to Equation (7).

7 MODEL PARAMETER ESTIMATION

The gold dissolution equations which were used to fit the model parameters to the experimental data are presented as follows:

$$\frac{dC_{Au}}{dt} = -k_1 C_{CN^-}^{\alpha} C_{O_2,s}^{\beta} A_i n \qquad \text{mol m}^{-3}\text{ s}^{-1} \qquad (54)$$

and

$$\frac{dC_{Au}}{dt} = -k_2 C_{CN^-}^{\alpha} C_{O_2,s}^{\beta} (C_{Au} - C_{Au}^{\infty})^{\gamma} A_i n \qquad \text{mol m}^{-3}\text{ s}^{-1} \qquad (55)$$

7.1 Experimental Data Available

The articles presented by Ling *et al*. (1996) and de Andrade Lima and Hodouin (2005) are used as sources for the experimental data in order to validate the studied models in this work. The experimental variables in Ling *et al*. (1996) were particle size, dissolved oxygen, cyanide and gold concentrations, as shown in Table 8. The temperature and pH were assumed to be constant at 20ºC and 11, respectively. The experiments were carried out in a 1 liter batch-type glass beaker reactor equipped with four Teflon coated baffles and a flat-blade turbine agitator. The agitation speed was maintained at 750 min^{-1}. The amount of ore was 600 g and the total slurry volume was around 800 ml. The dominant compositions of the ore are Na-feldspar ($NaAlSi_3O_8$), calcite ($CaCO_3$) and quartz (SiO_2).

Table 8 Experimental conditions in the data sets from Ling et al. (1996).

Data No.	**Mean Diameter, µm**	C_{CN^-} **, ppm**	C_{O_2} **, ppm**	C_{Au} **, ppm**
1	16.51	104	8.5	4.70
2	37.42	104	8.5	8.00
3	37.01	13	8.5	6.47
4	37.01	25	8.5	6.47
5	37.01	104	8.5	6.47
6	37.01	156	8.5	6.47
7	37.01	104	20	6.47
8	37.01	104	30	6.47
9	46.47	104	8.5	13.20

Table 9 Experimental conditions in the data sets from de Andrade Lima and Hodouin (2005).

Data No.	Mean Particle Diameter, μm	C_{CN^-}, ppm	C_{O_2}, ppm	C_{Au}, ppm
1	30	260	8	2.2
2	30	650	40	2.2
3	30	260	8	2.2
4	30	650	40	2.2
5	44	260	8	1.9
6	44	650	40	1.9
7	44	260	8	1.9
8	44	650	40	1.9
9	63	260	8	1.5
10	63	650	40	1.5
11	63	260	8	1.5
12	63	650	40	1.5
13	88	260	8	2.3
14	88	650	40	2.3
15	88	260	8	2.3
16	88	650	40	2.3
17	125	260	8	2.2
18	125	650	40	2.2
19	125	260	8	2.2
20	125	650	40	2.2
21	177	260	8	1.7
22	177	650	40	1.7
23	177	260	8	1.7
24	177	650	40	1.7

Table 9 presents the conditions of the experimental data from de Andrade Lima and Hodouin (2005). The experimental variables were the dissolved oxygen concentration, cyanide concentration and particle mean size as well. The temperature and pH were set to be constant at 20ºC and 12, respectively. The

experiments were carried out in a closed batch reactor of 1000 mL plastic beaker equipped with four baffles and four-blade turbine, in which 500 g of ore was added. The dominant components of the ore are quartz (SiO_2), clinochlore ($(Mg,Fe,Al)_6(Si,Al)_4O_{10}(OH)_8$ and illite ($(K,H_3O)Al_2Si_3AlO_{10}(OH)_2$).

7.2 Results and Discussions

The kinetic equation parameters were estimated by the Modest computer software (Haario, 2002) using the least squares method. The squared difference between the simulations and the experiments were minimized. The estimated parameters were obtained by fitting the model to the data. For the model presented in Equation (54), the estimated parameters consist of k_1, α, β and D_e, while parameters k_2 and γ are also estimated in the model of Equation (55). The estimated parameter values obtained from Equation (54) using experimental data shown in Table 8 are given below in Table 10.

Table 10 The estimated parameter values and their standard error from Equation (54)

Data Source	**Parameter**	**Values**	**Std. Error, %**
Ling *et al*. (1996)	k_1 $(m^3/mol)^{2.35}$ h^{-1}	0.555×10^{-5}	2603.8
Explained: 9.68%	α	2.29	27.1
	β	1.06	1838.9
	D_e (m^2/h)	0.101×10^{-8}	1147.2
de Andrade Lima and Hodouin (2005) Explained: 1.14%	k_1 $(mol/m^3)^{0.668}$ h^{-1}	0.114×10^{-6}	39.7
	α	0.32	44.4
	β	0.12×10^{-1}	703.6
	D_e (m^2/h)	0.610×10^{-7}	90475.6

The rate equation for gold cyanidation becomes:

$$r_s = 0.555\times10^{-5}\, C_{CN^-}^{2.29}\, C_{O_2,s}^{1.06} \qquad \text{mol m}^{-2}\ \text{h}^{-1} \qquad (56)$$

and $r_s = 0.114 \times 10^{-6} C_{CN^-}^{0.32} C_{O_2,s}^{0.012}$ mol m^{-2} h^{-1} (57)

Figure 40 demonstrates the fitting of the gold leaching model to the experimental data in both cases. The experimental data are given in Appendix IA. The fitted curves present the gold conversion on y-axis at any leaching time (h) on x-axis. The gold conversion can be calculated using:

$$\text{Conversion} = \frac{C_{Au,ini} - C_{Au}}{C_{Au,ini}} \quad (58)$$

where $C_{Au,ini}$ is the gold concentration in the solids at initial state (t = 0).

In Figure 40, the subfigures present the data sets from left to right starting from the upper-left corner. The coefficient of explanation of Figure 40 a) is 9.68%, meaning that the predicted values are not in good agreement with the experimental data. Figure 40 a) illustrates the overshooting taken place in the data sets no. 1, 5, 6, 7 and 8. The data sets no. 1 and 5 denote the experiments with small particle size compared to data sets no. 2 and 9. The cyanide concentration in the data set no. 6 is higher than in the other data sets. The data sets no. 7 and 8 have higher oxygen concentration than the others. This level of oxygen concentration in the solution might be in excess with respect to gold. In Figure 40 b), the coefficient of determination is only 1.14%. The prediction curves of the first twelve data sets containing small particle sizes indicate that there is some overshooting. These curves do not fit well to the experimental data, while the other curves containing larger size of particles show a better fit.

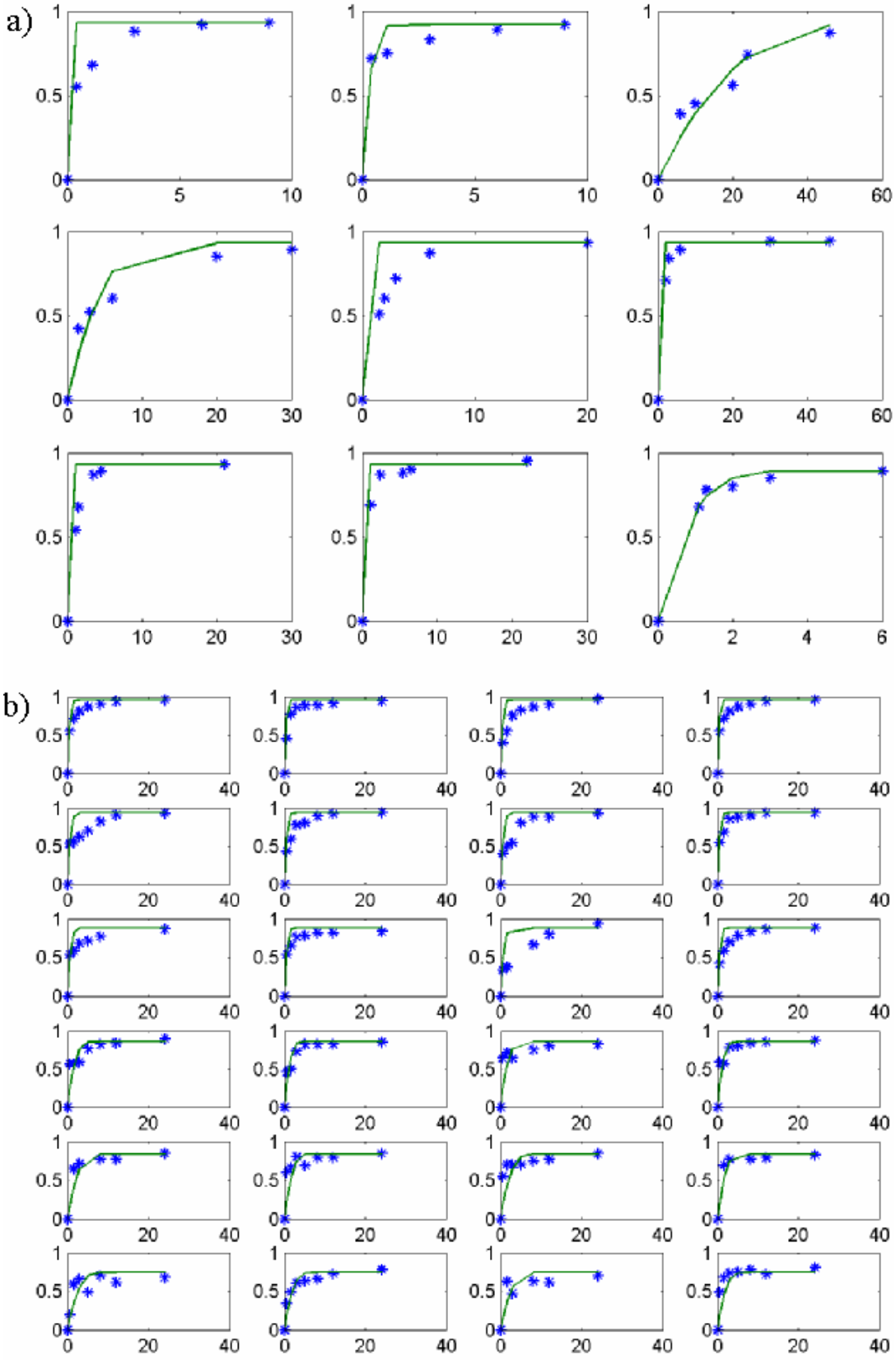

Figure 40 Gold conversion vs. time (h) for Equation (54); predicted conversion compared to experimental data; a) data from Ling *et al.* (1996); b) data from de Andrade Lima and Hodouin (2005).

The estimated parameters obtained for the gold leaching model shown in Equation (55) consist of k_2, α, β, γ and D_e for both data sources. These estimated parameters are given in Table 11.

Table 11 The estimated parameter values and their standard error for Equation (55).

Data Source	**Parameter**	**Values**	**Std. Error, %**
Ling *et al*. (1996)	$k_2\,(\mathrm{m^3/mol})^{2.731}\,\mathrm{h^{-1}}$	0.706×10^{-3}	63.9
Explained: 81.13%	α	1.38	9.4
	β	0.161	149.0
	γ	2.19	12.0
	$D_e\,(\mathrm{m^2/h_)}$	0.1×10^{-7}	416.8
de Andrade Lima and Hodouin (2005) Explained: 53.75%	$k_2\,(\mathrm{m^3/mol})^{2.011}\,\mathrm{h^{-1}}$	0.624×10^{-1}	167.6
	α	0.705	36.2
	β	0.16×10^{-1}	1012.4
	γ	2.29	12.2
	$D_e\,(\mathrm{m^2/h_)}$	0.515×10^{-9}	2.7×10^{5}

Therefore, the rate equation of gold cyanidation becomes:

$$r_s = 0.706\times10^{-3}\, C_{CN^-}^{1.38}\, C_{O_2,s}^{0.161}\, (C_{Au} - C_{Au}^{\infty})^{2.19} \qquad \mathrm{mol\ m^{-2}\ h^{-1}} \qquad (59)$$

and

$$r_s = 0.624\times10^{-1} C_{CN^-}^{0.705}\, C_{O_2,s}^{0.016}\, (C_{Au} - C_{Au}^{\infty})^{2.29} \qquad \mathrm{mol\ m^{-2}\ h^{-1}} \qquad (60)$$

Note that the unit for reagents and gold concentrations is $\mathrm{mol/m^3}$. The comparison of the model prediction and the experimental data is presented in Figure 41 for both data cases. The experimental data are given in Appendix IB. The coefficients of determination for Figure 41 a) and b) are 81.13% and 53.75%, respectively. The reaction order for the gold is approximately two, one for cyanide and between 0.0161-0.16 for the dissolved oxygen. The predicted curves fit to the experimental data quite well for both data cases and are also in obviously better agreement with

the data, when compared to the previous model, at any concentration of reagents and particle size. This implies that the gold leaching also depends on the gold concentration in the particles. Therefore, the term of the gold concentration difference between its current concentration and the residual concentration should not be omitted. The results also show that the gold leaching also depends on both cyanide and oxygen concentrations. Therefore, the form of Equation (25), should not be considered as the gold leaching rate equation. In addition, the obtained rate equation implies that the gold leaching rate is more sensitive to the cyanide concentration than oxygen concentration. In practice, it is not possible to completely leach all the gold from the particles which means that there is some amount of gold remained in the particles. Therefore, the gold concentration term in the model should not be considered as a constant. The rate equations, as shown in Equations (59) and (60) together with the mass balance equations for oxygen at the reacting surface as presented in Equations (52) and (53), show that the continually reduced reacting surface area has important effect on gold leaching. Therefore, the rate equations assuming the constant surface area, as presented in Equations (22) - (24), and rate equation without surface area consideration, as shown in Equation (26) should not be used to explain the gold leaching. Furthermore, the rate equation obtained in this work is not complicated as presented in Equation (28).

It is important that the developed models should be as reliable as possible. In a reliable model the estimated model parameters should be well identified without any severe cross-correlation between the parameters. The reliability of the estimated parameter can be analyzed by the Marcov chain Monte Carlo or MCMC methods. These methods use the numerical technique in Bayesian statistical analysis to analyze the nonlinear model. The MCMC methods present the probability distributions of the predicted parameters.

The reliability of the estimated parameters for both data cases is presented in Figure 42. The obtained effective diffusivity coefficient in Figure 42 is multiplied by internal scaling factor 1×10^{-6}. All parameters in Figure 42 a) and b) are almost well identified and there is no any cross-correlation between parameters. The posterior probability density distributions in Figure 42 a) appear sharp and the

distributions position is about in the center. Parameters k_2, α and γ in Figure 42 a) and parameter γ in Figure 42 b) have a narrow probability distribution. This can be also seen from Table 11 where the standard deviation value of these parameters is lower than the others. The parameters β in Figure 42 a) and k_2, α and β in Figure 42 b) are acceptable. The parameter D_e is not well-identified and shows relatively wide probability distribution increasing the uncertainty and standard deviation and thus affect to the accuracy of model. This is due to the fact that internal diffusion has no effect in gold leaching.

The significant of the internal diffusion to the gold leaching is also studied in this work. Figure 43 demonstrates the effect of internal diffusion as the ratio of the gold leaching rate with internal diffusion over the leaching rate without consideration of internal diffusion. Figure 43 a) shows that the curves steeply decrease at the beginning of leaching time and slightly increase later. From Figure 43 a), it could be explained that gold dissolves rapidly and forms passive layer fast in the beginning. After that the thickness of the passive layer is reduced showing the effect of internal diffusion becoming less and less important. It might be because there is only a small amount of gold on the surface to be leached resulting in thinner passive layer until the reaction has no internal diffusion effect (the ratio equals to 1). Figure 43 b) shows that the ratio is almost equal to 1 during the whole leaching time. This shows that there is no internal diffusion effect to be considered in the model. Therefore, the gold leaching is kinetically controlled by surface reaction.

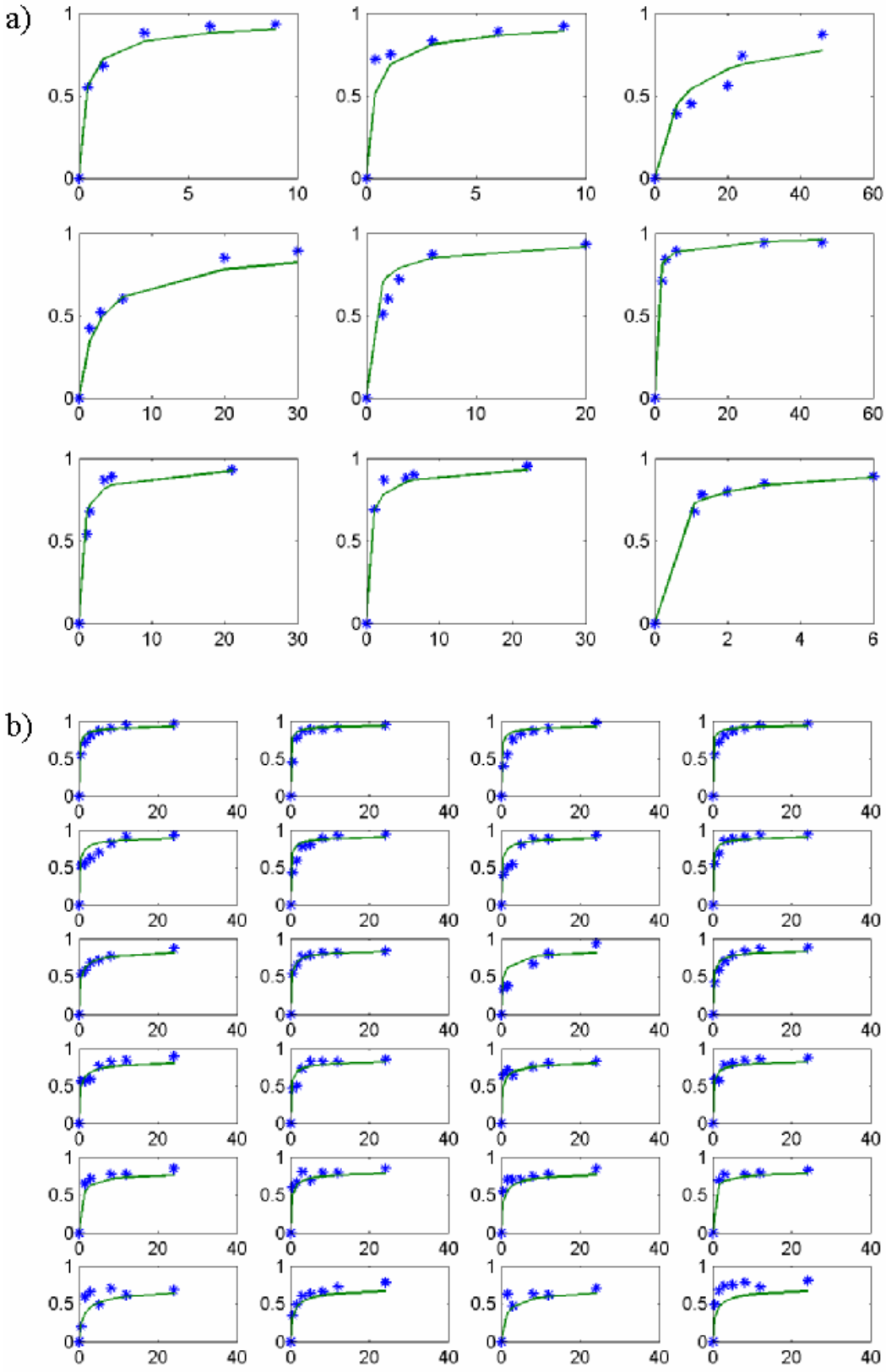

Figure 41 Gold conversion vs. time (h) for Equation (55); predicted conversion compared to experimental data; a) data from Ling *et al.* (1996); b) data from de Andrade Lima and Hodouin (2005).

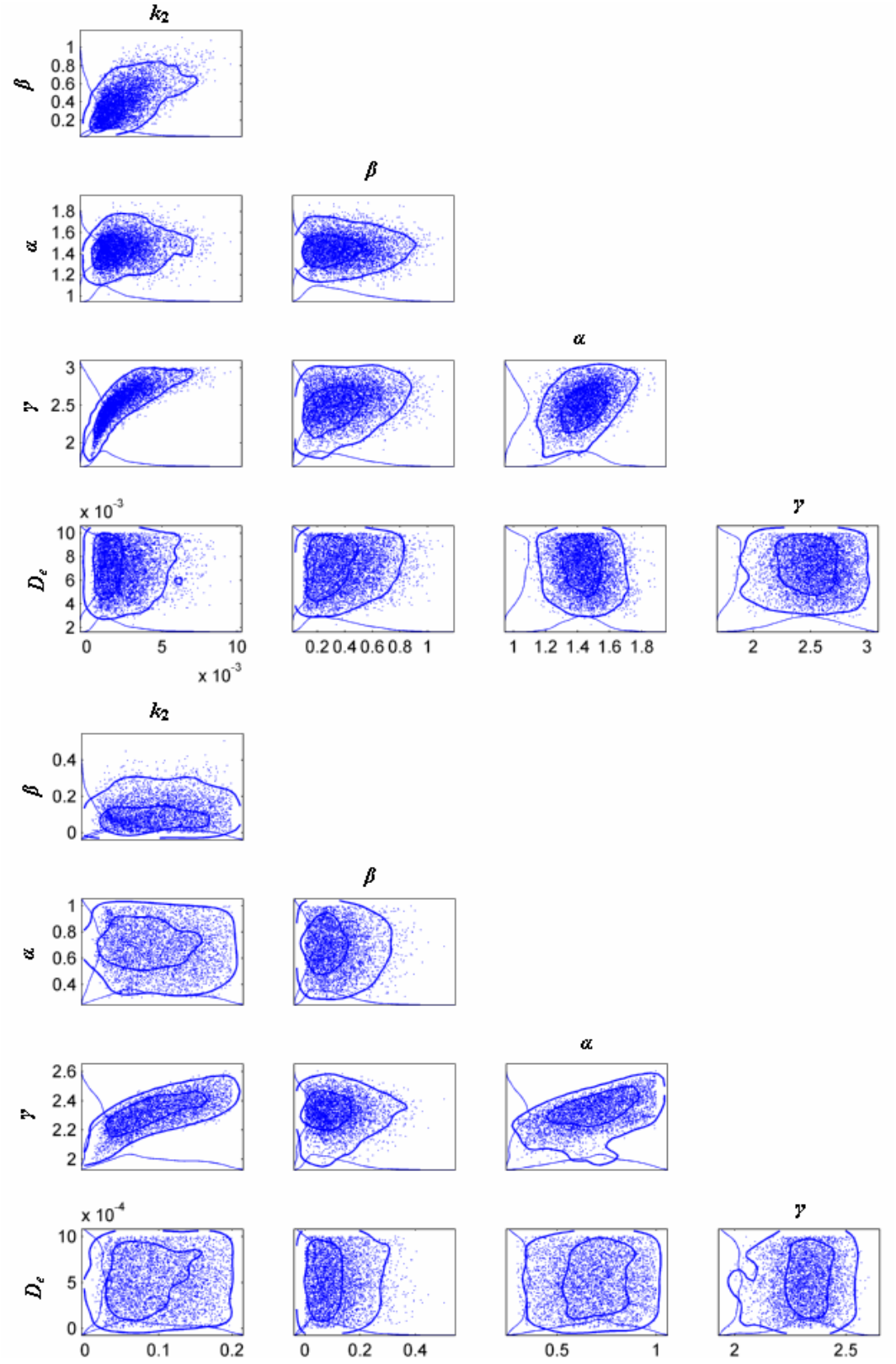

Figure 42 The two-dimensional probability distributions of the estimated parameters in Equation (55) from the MCMC analysis; a) data from Ling *et al*. (1996); b) data from de Andrade Lima and Hodouin (2005).

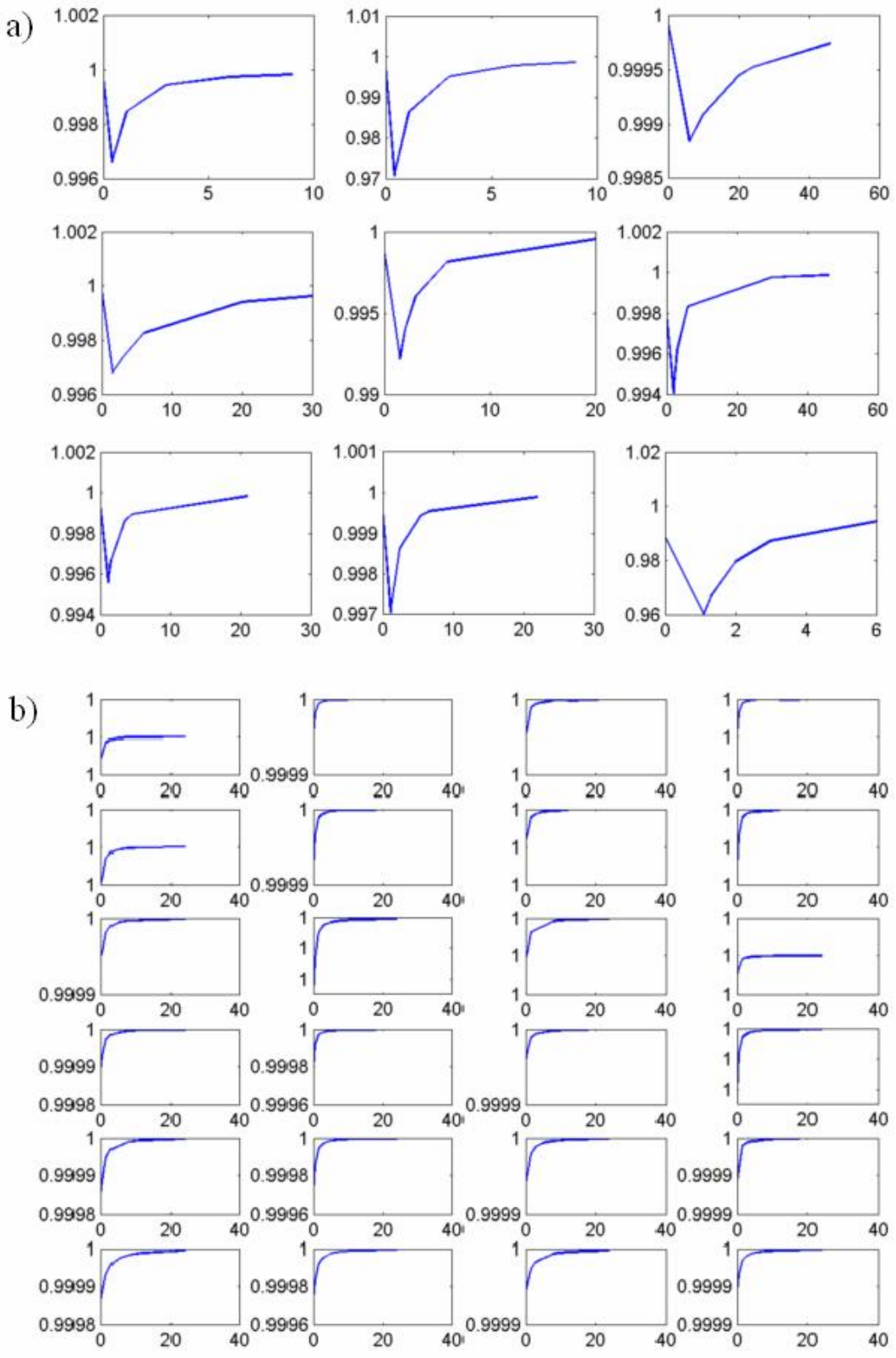

Figure 43 Effect of internal diffusion in Equation (55). Ratio of the actual gold leaching rate with / without internal diffusion consideration; a) data from Ling *et al.* (1996); b) data from de Andrade Lima and Hodouin (2005).

8 CONCLUSIONS

In this work the effect of leaching parameters on gold cyanidation has been studied. It is found that cyanide and dissolved oxygen concentration have a dominant effect on gold leaching. Increasing the reagents concentrations can improve gold dissolution rate. Small particle size plays a significant role to gold dissolution since it increases the area for surface reaction and the contacting area between solute and solution. Based on literature, the presence of other minerals, especially sulfide mineral, can retard the gold dissolution since they increase cyanide consumption. The oxidative processes can be used to treat them before leaching. Other parameters are found to slightly affect the gold cyanidation.

The parameters of the gold leaching models studied in this work were estimated by using the Modest computer software. A numerical shrinking-core model, together with simplifying approximations and assumptions, were developed for the simulation of gold leaching. The leaching parameters are the dissolved oxygen and cyanide concentrations and the difference of the gold concentration in the ore and the residual concentration in the ore after infinite leaching. The results show the advantage of using gold leaching model based on these parameters since the models take into account the effects of the reagent concentrations and the unreacted gold while the reduced reacting surface area is involved as well. However, the studied models have some limitations since side reactions, temperature and solid-liquid mass transfer resistances are not considered. The leaching parameters were estimated and fitted to the experimental data obtained from two different sources. The reliability of these parameters was studied by using the MCMC methods. The reliability can be seen from the cross-correlations and distributions of parameter and the standard deviations. The large standard error shows lacking sufficient reliability. The parameters α, β, γ and k_2 are more reliable than D_e in the case using data from Ling *et al.*, while γ is the most reliable in another case. The effect of internal diffusion as the ratio of the gold leaching rate with internal diffusion over the leaching rate without consideration of internal diffusion was also studied. The result shows that there is no internal diffusion

limitation, therefore the reaction is controlled by surface reaction. However, the reaction also depends on the gold concentration in the particles, as proposed. The reactive surface area is continuously reduced during leaching. Therefore the model considering the change of surface area is more accurate than the model assuming constant surface area. The rate equations including the estimated parameters are shown as follows:

$$r_s = 0.706\times10^{-3}\, C_{CN^-}^{1.38}\, C_{O_2,s}^{0.161}\, (C_{Au} - C_{Au}^{\infty})^{2.19} \qquad \text{mol m}^{-2}\,\text{h}^{-1}$$

and $$r_s = 0.624\times10^{-6} C_{CN^-}^{0.705}\, C_{O_2,s}^{0.016}\, (C_{Au} - C_{Au}^{\infty})^{2.29} \qquad \text{mol m}^{-2}\,\text{h}^{-1}$$

The rate equations show that the reaction orders are approximately two for gold, one for cyanide and a smaller value for oxygen. These reaction orders are at the same magnitude as those reported by Ling *et al*. (1996) and de Andrade Lima and Hodouin (2005). From the above equations, it is recognized that a unified kinetic model is difficult to establish since the nature of gold ores is complex. However, the proposed equations provide reasonable explanation. It can be concluded that the rate equation following Equation (43) is more reliable than other models presented in literature. This is because the reagents concentration, the particle size and the unreacted gold concentration are taken into account. Therefore the optimization of gold leaching should further be developed based on this equation. Additionally, more experimental data should be obtained in order to improve the model fitting.

For the future works, experiments should be done in stirred tank reactors under varying concentrations of reagents at constant temperature and pH in order to validate the model obtained in this work. Experiments should be also carried out in conditions where the effect of gas-liquid and solid-liquid mass transfer could be studied. Various types of ore containing different components of metal ions should be studied with this model as well. The latter study can be done under the optimal concentration of reagents at high pressure and/or high temperature in an autoclave in order to examine the effect of high pressure and temperature to the gold leaching.

REFERENCES

Aghamirian, M.M. & Yen, W.T. (2005) A Study of Gold Anodic Behavior in the Presence of Various Ions and Sulfide Menerals in cyanide Solution. *Minerals Engineering* Vol 18. pp. 89-102.

Breuer, P.L. Jeffrey, M.I. & Hewitt, D.M. (2008) Mechanisms of Sulfide Ion Oxidation during Cyanidation. Part I: The Effect of Lead (II) Ions. *Minerals Engineering*, Vol 21, pp. 579-586.

Brison, R.J. Elmore, C.L. & Mitchell, P. (1989) Utilization of Oxygen in Leaching and/or Recovery Procedures Employing Carbon. *United States Patent*, Mar 28 1989, No 4,816,234.

Campbell, J. & Watson, B. (2003) *Gravity Leaching with the Consep Acacia Reactor – Results from AngloGold Union Reefs.* Eighth Mill Operator's Conference, 21-23 July 2003.

Coetzee, J.W. & Grey, D.E. (1999) Counter-Current vs Co-Current Flow in Carbon-in-Pulp Adsorption Circuits. *Minerals Engineering*, Vol 12, No 4, pp. 415-422.

Consep Pty Ltd. *Consep Acacia Innovation in Process Technology*. [Brochure] http://www.consep.com.au/page13604324.aspx. [accessed 3 April 2008].

Corrans, I.J. & Angove, J.E. (1993) Activation of a Mineral Species. *United States Patent*, Aug 3 1993, No 5,232,491.

Crundwell, F.K. & Godorr, S.A. (1997) A Mathematical Model of the Leaching of Gold in Cyanide Solutions. *Hydrometallurgy*, Vol 44, pp. 147-162.

Dai, X. & Jeffrey, M.I. (2006) The Effect of Sulfide Minerals on the Leaching of Gold in Aerated Cyanide Solutions. *Hydrometallurgy*, Vol 82, pp. 118-125.

de Andrade Lima, L.R.P. & Hodouin, D. (2005) A Lumped Kinetic Model for Gold Ore Cyanidation. *Hydrometallurg*, Vol 79, pp. 121-137.

de Andrade Lima, L.R.P. & Hodouin, D. (2006) Simulation Study of the Optimal Distribution of Cyanide in a Gold Leaching Circuit. *Minerals Engineering*, Vol 19, pp. 1319-1327.

de Andrade Lima, L.R.P. (2007) Dynamic Simulation of the Carbon-in-Pulp and Carbon-in-Leach Processes. *Brazilian Journal of Chemical Engineering*, Vol 24, No 4, pp. 623-635.

Deschênes, G. & Wallingford G. (1995) Effect of Oxygen and Lead Nitrate on the Cyanidation of a Sulphide Bearing Gold Ore. *Minerals Engineering*, Vol 8, pp. 923-931.

Deschênes, G. & Prud'homme, P.J.H. (1997) Cyanidation of Copper-Gold Ore. *International Journal of Mineral Processing*, Vol 50, pp. 127-141.

Deschênes, G. et al (1998) Effect of the Composition of some Sulphide Minerals on Cyanidation and Use of Lead Nitrate and Oxygen to Alleviate their Impact. *Hydrometallurgy*, Vol 50, pp. 205-221.

Deschênes, G. et al. (2000) Effect if Lead Nitrate on Cyanidation of Gold Ores: Progress on the Study of the Mechanisms. *Minerals Engineering*, Vol 13, No 12, pp. 1263-1279.

Deschênes, G. Lacasse, S. & Fulton, M. (2003) Improvement of Cyanidation Practice at Goldcorp Red Lake Mine. *Minerals Engineering*, Vol 16, pp. 503-509.

Ellis, S. & Senanayake, G. (2004) The Effects of Dissolved Oxygen and Cyanide Dosage on Gold Extraction from a Pyrrhotite-Rich Ore. *Hydrometallurgy*, Vol 72, pp. 39-50.

Fan, Y. & Herz, R.K. (2007) Measurement and Enhancement of Gas–Liquid Mass Transfer in Milliliter-Scale Slurry Reactors. *Chemical Engineering Science*, Vol 62, pp. 5940-5951.

Fleming, C.A. (1992) Hydrometallurgy of Precious Metals Recovery. *Hydrometallurgy*, Vol 30, pp. 127-162.

Fleming, C.A. (2004) *Gold Extraction Technology Developments and their Implication to Profitability and Sustainability*. [Available at http://www.minecon.com/Proceedings04/Presentations/ChrisFlemingppt.pdf]

Garcia-Ochoa, F. & Gomez, E. (2004) Theoretical Prediction of Gas-Liquid Mass Transfer Coefficient, Specific Area and Hold-Up in Sparged Stirred Tanks. *Chemical Engineering Science*, Vol 59, pp. 2489-2501.

Gray, A.H. (2000*) Intensive Cyanidation and Its Implication for the Definition of Gravity Recoverable Gold.* Randol Gold & Silver Forum, Vancouver.

Hourn, M.M. Turner, D.W. & Holzberger, I.R. Atmospheric Mineral Leaching Process. *United States Patent*, Nov 30 1999, No 5,993,635.

Ibragimova, R.I. Mil'chenko, A.I. & Vorob'ev-Desyatovskii, N.V. (2007) Criteria for Choice of a Brand of Activated Carbon for Hydrometallurgical Recovery of Gold from Ore Pulps in Carbon-in-Leaching and Carbon-in-Pulp Processes. *Russian Journal of Applied Chemistry*, Vol 80, No 6, pp. 891-903.

Juvonen R. (1999) *Analysis of Gold and the Platinum Group Elements in Geological Samples*. Espoo: Geological survey of Finland.

Katsikaros, N. (2008) Re: *Questions regarding to ILR intensive cyanidation*. [NickK@gekkos.com] [sent on 29/07/2008].

Kondos, P.D. Deschênes, G. & Morrison, R.M. (1995) Process Optimization Studies in Gold Cyanidation. *Hydrometallurgy*, Vol 39, pp. 235-250.

Kunter, R.S. & Turney, J.R. (1986) Gold Recovery Process. *United States Patent*, Mar 25 1986, No 4,578,163.

Levenspiel, O. (1999) *Chemical Reaction Engineering*. 3rd Ed. Massachusetts: John Wiley & Sons.

Liebenberg, S.P. & Van Deventer, J.S.J. (1998) The Quantification of Shifting Adsorption Equilibria of Gold and Base Metals in CIP Plant. *Minerals Engineering*, Vol 11, No 6, pp. 551-562.

Ling, P. et al. (1996) An Improved Rate Equation for Cyanidation of a Gold Ore. *Canadian Metallurgical Quarterly*, Vol 35, No 3, pp. 225-234.

Longley, R.J. Katsikaros, N. & Hillman, C. (2002) *A New Age Gold Plant Flowsheet for the Treatment of High Grade Ores.* AusIMM-Metallurgical Plant Design and Operating Strategies Conference Aprill 2002.

Longley, R.J. McCallum, A. & Katsikaros, N. (2003) Intensive Cyanidation: Onsite Application of the InLine Leach Reactor to Gravity Gold Concentrates. *Minerals Engineering*, Vol 16, pp. 411-419.

Lorenzen, L. & Kleingeld A.W. (2000) New Generation Leaching Reactors for Effective Mass Transfer in Mineral Processing Operations. *Minerals Engineering*, Vol 13, pp. 1107-1115.

Lui, G.Q. & Yen, W.T. (1995) Effects of Sulphide Minerals and Dissolved Oxygen on the Gold and Silver Dissolution in Cyanide Solution. *Minerals Engineering*, Vol 8, pp. 111-123.

Marsden, J. & House, I. (1992) *The Chemistry of Gold Extraction*. West Sussex, England: Ellis Horwood.

McDougall, G. (1985) Recovery of Gold and/or Silver from Cyanide Leach Liquors on Activated Carbon. *United States Patent*, Jul 9 1985, No. 4,528,166.

Mineral Engineering International (2005) *Collaboration with Gravity Man Yields Gold*. [issued 09/05/2005] http://www.min-eng.com/gravityconcentration/85.html. [accessed 2 April 2008].

Nicol, M.J. Fleming C.A. & Cromberge, G. (1984) The Absorption of Gold Cyanide onto Activated Carbon. II. Application of the Kinetic Model to Multistage Absorption Circuits. *Journal of the South Africa Institute of Mining and Metallurgy*. Vol 81, No. 3, pp. 70-78.

Outokumpu (2004) *Gold Leaching Plant*
http://www.outotec.com/18960.epibrw. [accessed 10 April 2008].

Pangarkar, V.G. et al. (2002) Particle-Liquid Mass Transfer Coefficient in Two-/Three-Phase Stirred Tank Reactors. *Ind. Eng. Chem. Res.*, Vol 41, pp. 4141-4167.

Parga, J.R. Valenzuela, J.L. & Francisco, C.T. (2007) Pressure Cyanide Leaching for Precious Metals Recovery. *Aqueous Processing*, Oct 2007.

Rees, K.L. & van Deventer, J.S.J. (1999) The Role of Metal-Cyanide Species in Leaching Gold from a Copper Concentrate. *Minerals Engineering*, Vol 12, No. 8, pp. 877-892.

Rees, K.L. & van Deventer, J.S.J. (2000) Preg-Robbing Phenomena in the Cyanidation of Sulphide Ores. *Hydrometallurgy*, Vol 58, pp. 61-80.

Rees, K.L. & van Deventer, J.S.J. (2000) The Mechanism of Enhanced Gold Extraction from Ores in the Presence of Activated Carbon. Hydrometallurgy, Vol 58, pp. 151-167.

Senanayake, G. (2005) Kinetics and Reaction Mechanism of Gold Cyanidation: Surface Reaction Model via Au(I)-OH-CN Complexes. *Hydrometallurgy*, Vol 80, pp. 1-12.

Senanayake, G. (2008) A Review of Effects of Silver, Lead, Sulfide and Carbonaceous Matter on Gold Cyanidation and Mechanistic Interpretation. *Hydrometallurgy*, Vol 90, pp. 46-73.

Stange, W. (1999) The Process Design of Gold Leaching and Carbon-in-Pulp Circuits. *The Journal of the South Africa Institute of Mining and Metallurgy.*

Sundkvist, J.E. Recovery of Gold from Refractory Ores and Concentrates of Such Ores. *United States Patent*, Jul 2 2002, No 6,413,296 B1.

U.S. Environmental Protection Agency Office of Solid Waste (1993) *Cyanide Heap Leach and Tailings Impoundments Closure*. Washington, D.C., US.

van Deventer, J.S.J. Kam, K.M. & van de Walt, T.J. (2004) Dynamic Modelling of a Carbon-in-leach Process with the Regression Network. *Chemical Engineering Science*, Vol 59, pp. 4575-4589.

Vegter, N.M. (1992) The Distribution of Gold in Activated Carbon during Adsorption from Cyanide Solutions. *Hydrometallurgy*, Vol 30, pp. 229-242.

Vukcevic, S. (1997) The Mechanism of Gold Extraction and Copper Precipitation from Low Grade Ores in Cyanide Ammonia Systems. *Minerals Engineering*, Vol 10, No 3, pp. 309-326.

Wadsworth, M.E. et al. (2000) Gold Dissolution and Activation in Cyanide Solution. *Hydrometallurgy*, Vol 57, pp. 1-11.

Watson, B. & Steward, G. (2002) *Gravity Leaching-The ACACIA Reactor*. http://www.knelsongravitysolutions.com/sites/knelsongravity/files/reports/report36s.pdf.

Yalcin, M. & Arol, A.I. (2002) Gold Cyanide Adsorption Characteristics of Activated Carbon of Non-Coconut Shell Origin. *Hydrometallurgy*, Vol 63, pp. 201-206.

Zheng, J. et al. (1995) Study of Gold Leaching in Oxygenated Solutions Containing Cyanide-Copper-Ammonia Using a Rotating Quartz Crystal Microbalance. *Hydrometallurgy*, Vol 39, pp. 277-292.

APPENDICES

Appendix I

Experimental data from Ling et al. (1996) and de Andrade Lima and Hodouin (2005), showing gold conversion as presented in Figures 40 and 41

Appendix IA

Experimental data from Ling et al. (1996)

Appendix IB

Experimental data from de Andrade Lima and Hodouin (2005)

Appendix I (1/5) Experimental data from Ling et al. (1996) and de Andrade Lima and Hodouin (2005), showing gold conversion as presented in Figures 40 and 41

Appendix IA Experimental data from Ling et al. (1996)

Table I Gold conversion at any time for all data sets.

Data No.	Time (h)	Gold conversion	Data No.	Time (h)	Gold conversion	Data No.	Time (h)	Gold conversion
1	0.0	0.00	4	0.0	0.00	7	0.0	0.00
	0.4	0.55		1.5	0.42		1.1	0.54
	1.1	0.68		3.0	0.52		1.5	0.68
	3.0	0.88		6.0	0.60		3.5	0.87
	6.0	0.92		20.0	0.85		4.5	0.89
	9.0	0.93		30.0	0.89		21.0	0.93
2	0.0	0.00	5	0.0	0.00	8	0.0	0.00
	0.4	0.72		1.5	0.51		1.1	0.69
	1.1	0.75		2.0	0.60		2.4	0.87
	3.0	0.83		3.0	0.72		5.4	0.88
	6.0	0.89		6.0	0.87		6.5	0.90
	9.0	0.92		20.0	0.93		22.0	0.95
3	0.0	0.00	6	0.0	0.00	9	0.0	0.00
	6.0	0.39		2.0	0.71		1.1	0.68
	10.0	0.45		3.0	0.84		1.3	0.78
	20.0	0.56		6.0	0.89		2.0	0.80

Appendix I (2/5) Experimental data from Ling et al. (1996) and de Andrade Lima and Hodouin (2005), showing gold conversion as presented in Figures 40 and 41

Appendix IB Experimental data from de Andrade Lima and Hodouin (2005)

Table II Gold conversion at any time for all data sets.

Data No.	Time (h)	Gold conversion	Data No.	Time (h)	Gold conversion	Data No.	Time (h)	Gold conversion
1	0.0	0.00	3	0.0	0.00	5	0.0	0.00
	0.529	0.5455		0.529	0.4509		0.529	0.5263
	1.588	0.7159		1.588	0.7727		1.588	0.5568
	3.0	0.8105		3.0	0.8582		3.0	0.6184
	5.118	0.8673		5.118	0.8864		5.118	0.6974
	8.118	0.9055		8.118	0.8864		8.118	0.8221
	12.0	0.9432		12.0	0.9091		12.0	0.9079
	24.0	0.9623		24.0	0.9432		24.0	0.9316
2	0.0	0.00	4	0.0	0.00	6	0.0	0.00
	0.529	0.3941		0.529	0.5455		0.529	0.3947
	1.588	0.5455		1.588	0.7159		1.588	0.4932
	3.0	0.7536		3.0	0.8105		3.0	0.5395
	5.118	0.8295		5.118	0.8673		5.118	0.8026
	8.118	0.8673		8.118	0.9055		8.118	0.8816
	12.0	0.9055		12.0	0.9432		12.0	0.8816
	24.0	0.9718		24.0	0.9623		24.0	0.9274

Appendix I (3/5) Experimental data from Ling et al. (1996) and de Andrade Lima and Hodouin (2005), showing gold conversion as presented in Figures 40 and 41

Appendix IB Experimental data from de Andrade Lima and Hodouin (2005)

Table II Gold conversion at any time for all data sets (continued).

Data No.	Time (h)	Gold conversion	Data No.	Time (h)	Gold conversion	Data No.	Time (h)	Gold conversion
7	0.0	0.00	9	0.0	0.00	11	0.0	0.00
	0.529	0.4274		0.529	0.5333		0.529	0.5333
	1.588	0.5853		1.588	0.5833		1.588	0.6500
	3.0	0.7763		3.0	0.6833		3.0	0.7667
	5.118	0.8026		5.118	0.7167		5.118	0.7833
	8.118	0.8884		8.118	0.7747		8.118	0.8167
	12.0	0.9211		24.0	0.8667		12.0	0.8167
	24.0	0.9411					24.0	0.8333
8	0.0	0.00	10	0.0	0.00	12	0.0	0.00
	0.529	0.5395		0.529	0.333		0.529	0.4167
	1.588	0.6779		1.588	0.3747		1.588	0.5833
	3.0	0.8553		8.118	0.6667		3.0	0.7000
	5.118	0.8816		12.0	0.8000		5.118	0.7833
	8.118	0.9011		24.0	0.9333		8.118	0.8333
	12.0	0.9326					12.0	0.8667
	24.0	0.9326					24.0	0.8833

Appendix I (4/5) Experimental data from Ling et al. (1996) and de Andrade Lima and Hodouin (2005), showing gold conversion as presented in Figures 40 and 41

Appendix IB Experimental data from de Andrade Lima and Hodouin (2005)

Table II Gold conversion at any time for all data sets (continued).

Data No.	Time (h)	Gold conversion	Data No.	Time (h)	Gold conversion	Data No.	Time (h)	Gold conversion
13	0.0	0.00	15	0.0	0.00	17	0.0	0.00
	0.529	0.5652		0.529	0.4565		1.588	0.6505
	1.588	0.5652		1.588	0.4965		3.0	0.7168
	3.0	0.5870		3.0	0.7283		8.118	0.7727
	5.118	0.7643		5.118	0.8187		12.0	0.7727
	8.118	0.8187		8.118	0.8187		24.0	0.8464
	12.0	0.8387		12.0	0.8187			
	24.0	0.8913		24.0	0.8478			
14	0.0	0.00	16	0.0	0.00	18	0.0	0.00
	0.529	0.6378		0.529	0.5817		0.529	0.5455
	1.588	0.7100		1.588	0.5652		1.588	0.7027
	3.0	0.6378		3.0	0.7826		3.0	0.7027
	8.118	0.7517		5.118	0.8009		5.118	0.7027
	12.0	0.8009		8.118	0.8370		8.118	0.7518
	24.0	0.8187		12.0	0.8552		12.0	0.7727
				24.0	0.8730		24.0	0.8427

Appendix I (5/5) Experimental data from Ling et al. (1996) and de Andrade Lima and Hodouin (2005), showing gold conversion as presented in Figures 40 and 41

Appendix IB Experimental data from de Andrade Lima and Hodouin (2005)

Table II Gold conversion at any time for all data sets (continued).

Data No.	Time (h)	Gold conversion	Data No.	Time (h)	Gold conversion	Data No.	Time (h)	Gold conversion
19	0.0	0.00	21	0.0	0.00	23	0.0	0.00
	0.529	0.5977		0.529	0.1912		0.529	0.3382
	1.588	0.6659		1.588	0.5882		1.588	0.4853
	3.0	0.8077		3.0	0.6541		3.0	0.6029
	5.118	0.6855		5.118	0.4853		5.118	0.6324
	8.118	0.7900		8.118	0.7059		8.118	0.6618
	12.0	0.7900		12.0	0.6177		12.0	0.7206
	24.0	0.8427		24.0	0.6765		24.0	0.7794
20	0.0	0.00	22	0.0	0.00	24	0.0	0.00
	1.588	0.6941		1.588	0.6247		0.529	0.4853
	3.0	0.7727		3.0	0.4706		1.588	0.6765
	8.118	0.7727		8.118	0.6324		3.0	0.7353
	12.0	0.7900		12.0	0.6176		5.118	0.7500
	24.0	0.8250		24.0	0.7059		8.118	0.7794
							12.0	0.7206
							24.0	0.8088